

Scalable and accurate variational Bayes for high-dimensional binary regression models

Augusto Fasano*

Daniele Durante[†]Giacomo Zanella[†]

February 11, 2021

Abstract

Modern methods for Bayesian regression beyond the Gaussian response setting are computationally impractical or inaccurate in high dimensions. In fact, as discussed in recent literature, bypassing this trade-off is still an open problem even in routine binary regression models, and there is limited theory on the quality of variational approximations in high-dimensional settings. To address this gap, we study the approximation accuracy of routine-use mean-field variational Bayes solutions in high-dimensional probit regression with Gaussian priors, obtaining novel and practically relevant results on the pathological behavior of such strategies in uncertainty quantification, point estimation and prediction, that also suggest caution against maximum a posteriori estimates when $p > n$. Motivated by these results, we further develop a new partially-factorized variational approximation for the posterior distribution of the probit coefficients which leverages a representation with global and local variables but, unlike for classical mean-field assumptions, it avoids a fully factorized approximation, and instead assumes a factorization only for the local variables. We prove that the resulting approximation belongs to a tractable class of unified skew-normal densities that crucially incorporates skewness and, unlike for state-of-the-art mean-field solutions, converges to the exact posterior density as $p \rightarrow \infty$. To solve the variational optimization problem, we derive a tractable coordinate ascent variational inference algorithm that easily scales to p in tens of thousands, and provably requires a number of iterations converging to 1 as $p \rightarrow \infty$. Such findings are also illustrated in extensive empirical studies where our novel solution is shown to improve the approximation accuracy of mean-field variational Bayes for any n and p , with the magnitude of these gains being remarkable in those high-dimensional $p > n$ settings where state-of-the-art methods are computationally impractical.

Some key words: Bayesian computation; High-dimensional probit regression; Data augmentation; Variational Bayes; Truncated normal distribution; Unified skew-normal distribution

1 Introduction

The absence of a tractable posterior distribution in several Bayesian models and the recent abundance of high-dimensional datasets have motivated a growing interest in strategies for scalable learning of approximate posteriors, beyond classical sampling-based Markov chain Monte Carlo methods. Deterministic approximations, such as variational Bayes (Blei et al., 2017) and expectation-propagation (Minka, 2001), provide powerful and routinely-implemented solutions to improve computational efficiency in posterior inference. However, in high-dimensional models such methods still face open problems in terms of scalability, quality of the approximation and lack of theoretical support (Chopin and Ridgway, 2017; Blei et al., 2017).

Notably, such issues also arise in basic regression models for binary responses, which are routinely implemented and provide a key building block in several hierarchical models (e.g., Chipman et al., 2010; Rodriguez and Dunson, 2011). Recalling a recent review by Chopin and Ridgway (2017), the problem of posterior computation in binary regression is particularly challenging when the number of predictors p becomes large. Indeed, while standard sampling-based algorithms and accurate deterministic approximations can easily deal with small-to-moderate p problems, these strategies are impractical when p is large; e.g., $p > 1000$. As discussed by Blei et al. (2017), the solution to these scalability issues is typically obtained at the cost of lower accuracy in the approximation of the exact posterior distribution, and addressing this trade-off, both in theory and in

*ESOMAS Department, University of Turin, 10134 Turin, Italy, and Collegio Carlo Alberto, 10122 Turin, Italy, augusto.fasano@unito.it.

[†]Department of Decision Sciences and Institute for Data Science and Analytics, Bocconi University, 20136 Milan, Italy.

practice, is still an open area of modern research. In this article we prove, both theoretically and empirically, that in $p \gg n$ settings such a lower accuracy cost has dramatic implications not only in uncertainty quantification, but also in point estimation and prediction under routine-use mean-field variational Bayes approximations of the coefficients in probit models with Gaussian priors. To address this issue, we further develop a novel partially-factorized variational approximation for the posterior distribution of the probit coefficients which, unlike for most state-of-the-art solutions, crucially combines computational scalability and high accuracy, both theoretically and empirically, in large p settings, especially when $p > n$.

1.1 Bayesian computation for binary regression models

Classical specifications of Bayesian regression models for dichotomous data assume that the responses $y_i \in \{0; 1\}$, $i = 1, \dots, n$, are conditionally independent realizations from a Bernoulli variable $\text{Bern}[g(x_i^\top \beta)]$, given a fixed p -dimensional vector of predictors $x_i = (x_{i1}, \dots, x_{ip})^\top \in \mathbb{R}^p$, $i = 1, \dots, n$, and the associated coefficients $\beta = (\beta_1, \dots, \beta_p)^\top \in \mathbb{R}^p$. The mapping $g(\cdot) : \mathbb{R} \rightarrow (0, 1)$ is commonly specified to be either the logit or probit link, thus obtaining $\text{pr}(y_i = 1 | \beta) = [1 + \exp(-x_i^\top \beta)]^{-1}$ in the first case, and $\text{pr}(y_i = 1 | \beta) = \Phi(x_i^\top \beta)$ in the second, where $\Phi(\cdot)$ is the cumulative distribution function of a standard normal. In performing Bayesian inference under these models, it is common practice to specify Gaussian priors for the coefficients in β , and then update such priors with the likelihood of the observed data $y = (y_1, \dots, y_n)^\top$ to obtain the posterior $p(\beta | y)$, which is used for point estimation, uncertainty quantification and prediction. However, the apparent lack of conjugacy motivates computational methods relying either on Monte Carlo integration or deterministic approximations (Chopin and Ridgway, 2017).

A popular class of Markov chain Monte Carlo methods that has been widely used in Bayesian regression models for binary data leverages augmented data representations which allow the implementation of tractable Gibbs samplers relying on conjugate full-conditional distributions. In Bayesian probit regression this strategy exploits the possibility of expressing the binary data $y_i \in \{0; 1\}$, $i = 1, \dots, n$, as dichotomized versions of an underlying regression model for Gaussian responses $z_i \in \mathbb{R}$, $i = 1, \dots, n$, thereby restoring conjugacy between the Gaussian prior for the coefficients in β and the augmented data z_i , which are in turn sampled from truncated normal full-conditionals (Albert and Chib, 1993). More recently, Polson et al. (2013) proposed a related strategy for logit regression which is based on a representation of the logistic likelihood as a scale mixture of Gaussians with respect to Pólya-gamma augmented variables $z_i \in \mathbb{R}^+$, $i = 1, \dots, n$. Despite their simplicity, these methods face well-known computational and mixing issues in high-dimensional settings, especially with imbalanced datasets (Johndrow et al., 2019). We refer to Chopin and Ridgway (2017) for a discussion of related data-augmentation strategies (Holmes and Held, 2006; Frühwirth-Schnatter and Frühwirth, 2007) and alternative sampling methods (e.g., Haario et al., 2001; Hoffman and Gelman, 2014). While these strategies address some issues of data-augmentation samplers, they are still computationally impractical in large p settings (e.g., Chopin and Ridgway, 2017; Nishimura and Suchard, 2018; Durante, 2019).

An exception to the above methods is provided by the recent contribution of Durante (2019), which proves that in Bayesian probit regression with Gaussian priors the posterior actually belongs to the class of unified skew-normal (SUN) distributions (Arellano-Valle and Azzalini, 2006). These variables have several closure properties which facilitate posterior inference in large p settings. However, the calculation of relevant functionals for inference and prediction requires the evaluation of cumulative distribution functions of n -variate Gaussians or sampling from n -variate truncated normals, thus making these results impractical in a variety of applications with sample size n greater than a few hundreds (Durante, 2019).

A possible solution to scale-up computations is to consider deterministic approximations of the posterior distribution. In binary regression, two popular strategies are expectation-propagation (Chopin and Ridgway, 2017) and mean-field variational Bayes based on global and local variables (Jaakkola and Jordan, 2000; Consonni and Marin, 2007; Durante and Rigon, 2019); see Riihimäki et al. (2013) and Girolami and Rogers (2006) for an extension of such strategies to multinomial models with Gaussian process priors. The first class of methods relies on a Gaussian approximation of the exact posterior distribution $p(\beta | y)$ which yields notable approximation accuracy via a moment matching of approximate marginals that have the same factorized form of the actual posterior. These accuracy gains come, however, with a computational cost that limits the applicability of expectation-propagation to settings with moderate p (e.g., Chopin and Ridgway, 2017). Indeed, recalling a concluding remark by Chopin and Ridgway (2017), the lack of scalability to large p (e.g., $p > 1000$) is common to most state-of-the-art accurate methods for Bayesian computation in binary regression, including also Knowles and Minka (2011); Marlin et al. (2011), among others.

Mean-field variational Bayes with global and local variables addresses the computational bottlenecks of expectation-propagation by approximating the posterior density $p(\beta, z | y)$ for the global parameters $\beta = (\beta_1, \dots, \beta_p)^\top$ and the local augmented data $z = (z_1, \dots, z_n)^\top$ with an optimal factorized density $q_{\text{MF}}^*(\beta) \prod_{i=1}^n q_{\text{MF}}^*(z_i)$ which is the closest in Kullback–Leibler divergence (Kullback and Leibler, 1951) to $p(\beta, z | y)$, among all the approximating densities in the mean-field family $\mathcal{Q}_{\text{MF}} = \{q_{\text{MF}}(\beta, z) : q_{\text{MF}}(\beta, z) = q_{\text{MF}}(\beta)q_{\text{MF}}(z)\}$. Optimization typically proceeds via coordinate ascent variational methods which scale easily to large p settings. However, the mean-field class underestimates posterior uncertainty and often leads to Gaussian approximations affecting quality of inference if the posterior is non-Gaussian (Kuss and Rasmussen, 2005).

In Section 2.1, we deepen the above results by proving that, in the context of high-dimensional probit regression with Gaussian priors, the mean-field assumption has dramatic implications not only in uncertainty quantifications, but also in point estimation and, as a direct consequence, in prediction. In particular, we show that, as $p \rightarrow \infty$, with fixed n , the mean-field solution overshinks the location of the exact posterior distribution and yields to an excessively rapid concentration of the predictive probabilities around 0.5, thereby leading to unreliable inference and prediction. While there has been a recent focus in the literature on studying frequentist consistency properties of mean-field variational approximations (Wang and Blei, 2019; Ray and Szabó, 2020; Yang et al., 2020), there is much less theory on the accuracy in approximating the exact posterior distribution in high dimensions. Our results in this direction yields novel and practically relevant findings, while motivating improved approximations, as discussed below.

To address the issues highlighted in Section 2.1, we propose in Section 2.2 a novel partially-factorized variational approximation for Bayesian probit regression which crucially drops the classical mean-field independence assumption between the global variables β and the augmented data z . Unlike for standard implementations of expectation-propagation (Chopin and Ridgway, 2017) and Hamiltonian Monte Carlo methods (Hoffman and Gelman, 2014), the proposed solution scales easily to $p \gg 1000$ settings, while, differently from the computational strategies proposed in Durante (2019), it only requires the evaluation of distribution functions of univariate Gaussians. Moreover, despite having a computational cost comparable to standard mean-field methods for probit models (Consonni and Marin, 2007), the proposed solution leads to a substantially improved approximation of the posterior distribution which crucially incorporates skewness, and effectively reduces bias in locations, variances and predictive probabilities, especially in $p > n$ settings. In fact, we prove that the error made by the partially-factorized variational solution in approximating the exact posterior density goes to 0 as $p \rightarrow \infty$. Optimization proceeds via a simple and scalable coordinate ascent variational algorithm which provides a tractable SUN approximating density and requires a number of iterations to find the optimum that converges to 1 as $p \rightarrow \infty$. The performance of the proposed methods is illustrated in extensive simulation studies in Section 3, and in a high-dimensional Alzheimer’s application in Section 4, with $p = 9036$, where posterior inference under our proposed solution requires only few seconds. These quantitative assessments confirm that the empirical performance of the newly proposed strategy closely matches what expected from theory, even in settings beyond our assumptions. In addition, such studies highlight that the proposed solution is orders of magnitude faster than state-of-the-art accurate methods in high-dimensional settings, and, unlike for classical mean-field methods, pays almost no cost in inference accuracy and predictive performance, when $p > n$. To our knowledge, available solutions in the literature do not provide such an effective combination of scalability and accuracy in high dimensions. Concluding remarks, proofs and additional studies can be found in Section 5 and in the Supplementary Materials where we also discuss the computational complexity of the proposed inference and optimization strategies which can be performed at a $\mathcal{O}(pn \cdot \min\{p, n\})$ overall cost. Codes and tutorials to implement the methods and reproduce the analyses are available at <https://github.com/augustofasano/Probit-PFMVB>.

2 Approximate Bayesian Inference for Probit Models

Recalling Section 1, we focus on posterior inference for the classical Bayesian probit model

$$(y_i | \beta) \sim \text{Bern}[\Phi(x_i^\top \beta)], \quad (i = 1, \dots, n), \quad \text{with } \beta \sim \text{N}_p(0, \nu_p^2 I_p). \quad (1)$$

In (1), each y_i is a Bernoulli variable whose success probability depends on the p -dimensional vector of observed predictors $x_i = (x_{i1}, \dots, x_{ip})^\top$ under a probit mapping. The coefficients $\beta = (\beta_1, \dots, \beta_p)^\top$ regulate the effect of each predictor and are assigned independent Gaussian priors $\beta_j \sim \text{N}(0, \nu_p^2)$, for each $j = 1, \dots, p$. Besides providing a default specification, these priors are also key building-blocks which can be naturally extended to general scale mixtures of Gaussians.

Note also that, although our contribution can be naturally generalized to a generic multivariate Gaussian prior for β , we consider here the common setting with $\beta \sim \mathcal{N}_p(0, \nu_p^2 I_p)$ to ease notation, and allow the prior variance ν_p^2 to possibly change with p . This choice incorporates not only routine implementations of Bayesian probit models relying on constant prior variances $\nu_p^2 = \nu^2$ for the coefficients (e.g., [Chopin and Ridgway, 2017](#)), but also more structured formulations for high-dimensional problems which define $\nu_p^2 = \nu^2/p$ to control prior variance of the entire linear predictor and induce increasing shrinkage (e.g., [Simpson et al., 2017](#); [Fuglstad et al., 2018](#)); see [Assumption 2](#) for details on the asymptotic behavior of ν_p^2 .

Model (1) also has a simple constructive representation relying on Gaussian augmented data, which has been broadly used in the development of sampling-based ([Albert and Chib, 1993](#)) and variational ([Consonni and Marin, 2007](#); [Girolami and Rogers, 2006](#)) methods. More specifically, (1) can be obtained by marginalizing out the augmented data $z = (z_1, \dots, z_n)^\top$ in the model

$$y_i = 1(z_i > 0), \text{ with } (z_i | \beta) \sim \mathcal{N}(x_i^\top \beta, 1), \quad (i = 1, \dots, n), \quad \text{and } \beta \sim \mathcal{N}_p(0, \nu_p^2 I_p). \quad (2)$$

Recalling [Albert and Chib \(1993\)](#), the above construction leads to closed-form full-conditionals for β and z , thus allowing the implementation of a Gibbs sampler where $p(\beta | z, y) = p(\beta | z)$ is a Gaussian density, and each $p(z_i | \beta, y) = p(z_i | \beta, y_i)$ is the density of a truncated normal, for $i = 1, \dots, n$. We refer to [Albert and Chib \(1993\)](#) for more details on this strategy. Our focus here is on large p settings where classical Markov chain Monte Carlo methods are often impractical, thus motivating more scalable methods relying on approximate posteriors. In [Section 2.1](#), we discuss standard mean-field strategies for Bayesian probit models ([Consonni and Marin, 2007](#)) which rely on representation (2), and prove that in $p \gg n$ settings these approaches yield poor approximations of the exact posterior that underestimate not only the variance but also the location, thus leading to unreliable inference and prediction. In [Section 2.2](#), we address these issues via a new partially-factorized variational approximation that has substantially improved practical and theoretical performance in large p settings, especially when $p > n$.

2.1 Mean-field variational Bayes with global and local variables

Recalling [Blei et al. \(2017\)](#), mean-field variational Bayes with global and local variables aims at providing a tractable approximation for the joint posterior density $p(\beta, z | y)$ of the global parameters $\beta = (\beta_1, \dots, \beta_p)^\top$ and the local variables $z = (z_1, \dots, z_n)^\top$, within the mean-field class of factorized densities $\mathcal{Q}_{\text{MF}} = \{q_{\text{MF}}(\beta, z) : q_{\text{MF}}(\beta, z) = q_{\text{MF}}(\beta)q_{\text{MF}}(z)\}$. The optimal solution $q_{\text{MF}}^*(\beta)q_{\text{MF}}^*(z)$ within this family is the one that minimizes the Kullback–Leibler (KL) divergence ([Kullback and Leibler, 1951](#)) defined as

$$\text{KL}[q_{\text{MF}}(\beta, z) || p(\beta, z | y)] = E_{q_{\text{MF}}(\beta, z)}[\log q_{\text{MF}}(\beta, z)] - E_{q_{\text{MF}}(\beta, z)}[\log p(\beta, z | y)], \quad (3)$$

with $q_{\text{MF}}(\beta, z) \in \mathcal{Q}_{\text{MF}}$. Alternatively, it is possible to obtain $q_{\text{MF}}^*(\beta)q_{\text{MF}}^*(z)$ by maximizing

$$\text{ELBO}[q_{\text{MF}}(\beta, z)] = E_{q_{\text{MF}}(\beta, z)}[\log p(\beta, z, y)] - E_{q_{\text{MF}}(\beta, z)}[\log q_{\text{MF}}(\beta, z)], \quad q_{\text{MF}}(\beta, z) \in \mathcal{Q}_{\text{MF}}, \quad (4)$$

since the ELBO coincides with the negative KL up to an additive constant. Recall also that the KL divergence is always non-negative and refer to [Armagan and Zaretzki \(2011\)](#) for the expression of $\text{ELBO}[q_{\text{MF}}(\beta, z)]$ under (2). The maximization of (4) is typically easier and can be performed via a coordinate ascent variational inference algorithm (e.g., [Blei et al., 2017](#)) cycling among steps

$$q_{\text{MF}}^{(t)}(\beta) \propto \exp\{E_{q_{\text{MF}}^{(t-1)}(z)} \log[p(\beta | z, y)]\}, \quad q_{\text{MF}}^{(t)}(z) \propto \exp\{E_{q_{\text{MF}}^{(t)}(\beta)} \log[p(z | \beta, y)]\} \quad (5)$$

where $q_{\text{MF}}^{(t)}(\beta)$ and $q_{\text{MF}}^{(t)}(z)$ are the solutions at iteration t . We refer to [Blei et al. \(2017\)](#) for why the updating in (5) iteratively optimizes the ELBO in (4), and highlight here how (5) is particularly simple to implement in Bayesian models with tractable full-conditional densities $p(\beta | z, y)$ and $p(z | \beta, y)$. This is the case of the augmented-data representation (2) for model (1). Indeed, recalling [Albert and Chib \(1993\)](#) it easily follows that the full-conditionals in model (2) are

$$\begin{aligned} (\beta | z, y) &\sim \mathcal{N}_p(VX^\top z, V), \quad V = (\nu_p^{-2}I_p + X^\top X)^{-1}, \\ (z_i | \beta, y) &\sim \text{TN}(x_i^\top \beta, 1, \mathbb{A}_{z_i}), \quad (i = 1, \dots, n), \end{aligned} \quad (6)$$

where X is the $n \times p$ design matrix with rows x_i^\top , whereas $\text{TN}(x_i^\top \beta, 1, \mathbb{A}_{z_i})$ denotes a univariate normal distribution having mean $x_i^\top \beta$, variance 1, and truncation to the interval $\mathbb{A}_{z_i} = \{z_i : (2y_i - 1)z_i > 0\}$. A key consequence of the conditional independence of z_1, \dots, z_n , given β and y , is that $q_{\text{MF}}^{(t)}(z) = \prod_{i=1}^n q_{\text{MF}}^{(t)}(z_i)$ and thus the optimal mean-field solution always factorizes as $q_{\text{MF}}^*(\beta)q_{\text{MF}}^*(z) = q_{\text{MF}}^*(\beta) \prod_{i=1}^n q_{\text{MF}}^*(z_i)$. Replacing the densities of the above full-conditionals in

Algorithm 1. Steps of the procedure to obtain $q_{\text{MF}}^*(\beta, z) = q_{\text{MF}}^*(\beta) \prod_{i=1}^n q_{\text{MF}}^*(z_i)$

[1] Initialize $\bar{z}^{(0)} = (\bar{z}_1^{(0)}, \dots, \bar{z}_n^{(0)})^\top \in \mathfrak{R}^n$.

[2] **for** t from 1 until convergence of $\text{ELBO}[q_{\text{MF}}^{(t)}(\beta, z)]$ **do**

Set $\bar{\beta}^{(t)} = VX^\top \bar{z}^{(t-1)}$.

Set $\bar{z}^{(t)} = (\bar{z}_1^{(t)}, \dots, \bar{z}_n^{(t)})^\top$ with

$\bar{z}_i^{(t)} = x_i^\top \bar{\beta}^{(t)} + (2y_i - 1)\phi(x_i^\top \bar{\beta}^{(t)}) / \Phi[(2y_i - 1)x_i^\top \bar{\beta}^{(t)}], (i = 1, \dots, n)$.

Output: $q_{\text{MF}}^*(\beta, z) = \phi_p(\beta - \bar{\beta}^*; V) \prod_{i=1}^n \phi(z_i - x_i^\top \bar{\beta}^*) \Phi[(2y_i - 1)x_i^\top \bar{\beta}^*]^{-1} 1[(2y_i - 1)z_i > 0]$.

(5), it can be easily noted that $q_{\text{MF}}^*(\beta)$ and $q_{\text{MF}}^*(z_i), i = 1, \dots, n$, are Gaussian and truncated normal densities, respectively, with parameters as in Algorithm 1 (Consonni and Marin, 2007). Note that the parametric form of the optimal approximating densities follows directly from (5)–(6), without pre-specifying it, and that in Algorithm 1 the generic quantity $\phi_p(\beta - \mu; \Sigma)$ represents the density of a p -variate Gaussian for β with mean μ and variance-covariance matrix Σ .

Algorithm 1 relies on simple operations which basically require only to update $\bar{\beta}^{(t)}$ via matrix operations, and, unlike for most state-of-the-art alternative strategies, is computationally feasible in high-dimensional settings; see e.g., Table 1. Due to the Gaussian form of $q_{\text{MF}}^*(\beta)$ also the calculation of the approximate posterior moments and predictive probabilities is straightforward. The latter quantities can be easily expressed as

$$\text{pr}_{\text{MF}}(y_{\text{NEW}} = 1 | y) = E_{q_{\text{MF}}^*(\beta)}[\Phi(x_{\text{NEW}}^\top \beta)] = \Phi[x_{\text{NEW}}^\top \bar{\beta}^* (1 + x_{\text{NEW}}^\top V x_{\text{NEW}})^{-1/2}], \quad (7)$$

where $x_{\text{NEW}} \in \mathfrak{R}^p$ are the covariates of the new unit, and $\bar{\beta}^* = E_{q_{\text{MF}}^*(\beta)}(\beta)$. However, as shown by the asymptotic results in Theorem 1, the mean-field solution can lead to poor approximations of the posterior in high dimensions as $p \rightarrow \infty$, causing concerns on the quality of inference and prediction. These asymptotic results are derived under the following random design assumption.

Assumption 1 Assume that the predictors $x_{ij}, i = 1, \dots, n, j = 1, \dots, p$, are independent random variables with $E(x_{ij}) = 0, E(x_{ij}^2) = \sigma_x^2$ and $E(x_{ij}^4) \leq c_x$ for some $c_x < \infty$.

The above random design assumption is common to asymptotic studies of regression models (e.g., Reiß, 2008; Qin and Hobert, 2019). Moreover, the zero mean and constant variance assumption is a natural requirement in binary regression, where the predictors are typically standardized following the recommended practice (Gelman et al., 2008; Chopin and Ridgway, 2017). In Section 2.2, we will relax Assumption 1 to prove that the proposed partially-factorized solution has desirable asymptotic properties even in more general settings including some dependence in the rows and columns of X . Since the mean-field approximation has pathological asymptotic behaviors even under complete independence assumptions, we avoid such a relaxation in Theorem 1 to simplify presentation. We shall also emphasize that, as illustrated in Sections 3–4 and in the Supplementary Materials, the empirical evidence on simulated and real data, where our assumptions might not hold, is coherent with the theory results stated in the article. To rule out pathological cases, we also require the following mild technical assumption on the behavior of ν_p^2 as $p \rightarrow \infty$.

Assumption 2 Assume that $\sup_p \{\nu_p^2\} < \infty$ and $\lim_{p \rightarrow \infty} p\nu_p^2 = \alpha \in (0, \infty]$.

Observe that Assumption 2 includes the two elicitations for ν_p^2 of interest in these settings as discussed in Section 2; i.e., $\nu_p^2 = \nu^2$ and $\nu_p^2 = \nu^2/p$, with $\nu^2 < \infty$. In the following, we use the convention $\alpha\sigma_x^2(1 + \alpha\sigma_x^2)^{-1} = 1 = (1 + \alpha\sigma_x^2)(\alpha\sigma_x^2)^{-1}$, whenever $\alpha = \infty$. Throughout the paper, n is assumed be fixed while $p \rightarrow \infty$.

Theorem 1 Under Assumption 1–2: (a) $\liminf_{p \rightarrow \infty} \text{KL}[q_{\text{MF}}^*(\beta) || p(\beta|y)] > 0$ almost surely (a.s.). Moreover, (b) $\nu_p^{-1} \|E_{q_{\text{MF}}^*(\beta)}(\beta)\| \xrightarrow{\text{a.s.}} 0$ as $p \rightarrow \infty$, where $\|\cdot\|$ denotes the Euclidean norm. On the contrary, $\nu_p^{-1} \|E_{p(\beta|y)}(\beta)\| \xrightarrow{\text{a.s.}} [\alpha\sigma_x^2(1 + \alpha\sigma_x^2)^{-1}]^{1/2} c\sqrt{n} > 0$ when $p \rightarrow \infty$, where $c = 2 \int_0^\infty z\phi(z)dz$ is a strictly positive constant. Finally, (c) $\liminf_{p \rightarrow \infty} \sup_{x_{\text{NEW}} \in \mathfrak{R}^p} |\text{pr}_{\text{MF}}(y_{\text{NEW}} = 1 | y) - \text{pr}(y_{\text{NEW}} = 1 | y)| > 0$ a.s., as $p \rightarrow \infty$, where $\text{pr}(y_{\text{NEW}} = 1 | y) = E_{p(\beta|y)}[\Phi(x_{\text{NEW}}^\top \beta)]$ denote the exact posterior predictive probability for a new unit with predictors $x_{\text{NEW}} \in \mathfrak{R}^p$.

According to Theorem 1(a)–1(b), the mean-field solution causes over-shrinkage of approximate posterior means, that can result in an unsatisfactory approximation of the whole posterior density $p(\beta | y)$ in high dimensions. For instance, combining Theorem 1(b) and (7), the over-shrinkage of $\bar{\beta}^*$ towards 0 may cause an excessively rapid concentration of $\text{pr}_{\text{MF}}(y_{\text{NEW}} = 1 | y)$ around 0.5, thereby inducing bias; see Theorem 1(c). As we will show with extensive empirical studies in

Sections 3–4, the magnitude of this bias can be dramatic in high dimensions. In addition, although as $p \rightarrow \infty$ the prior plays a progressively more important role in the Bayesian updating, Theorem 1(b) suggests that even few data points can induce non-negligible differences between prior and posterior moments such as, for example, the expectations. As shown in Theorem 2 such issues can be provably solved by the partially-factorized solution we propose in Section 2.2.

Remark 1 *As discussed in the proof of Theorem 1 and in Armagan and Zaretski (2011), $\bar{\beta}^*$ is also the mode of the actual posterior $p(\beta | y)$ and, hence, it also coincides with the ridge estimate in probit regression. Therefore, the above results suggest that, despite its popularity (Chopin and Ridgway, 2017; Gelman et al., 2008), the posterior mode should be avoided as a point estimate in $p \gg n$ settings. As a direct consequence, also Laplace approximation would provide unreliable inference since this approximation is centered at the posterior mode.*

The above results are in apparent contrast with the fact that the marginal posterior densities $p(\beta_j | y)$ often exhibit negligible skewness and their modes $\arg \max_{\beta_j} p(\beta_j | y)$ tend to be close to the corresponding mean $E_{p(\beta_j|y)}(\beta_j)$; see e.g., Figure S2 in the Supplementary Materials. However, the same is not true for the joint posterior density $p(\beta | y)$, where little skewness is sufficient to induce dramatic differences between the joint posterior mode, $\arg_{\beta} \max p(\beta|y)$, and the posterior expectation; see e.g., Figure 3. In this sense, the results in Theorem 1 point towards caution in assessing Gaussianity of high-dimensional distributions based on the shape of the marginals.

Motivated by the above considerations, in Section 2.2 we develop a new partially-factorized variational strategy with global and local variables that solves the aforementioned issues without increasing the computational cost. In fact, the cost of our procedure is the same of the classical mean-field one but, unlike for such a strategy, we obtain a substantially improved approximation whose distance from the exact posterior goes to 0 as $p \rightarrow \infty$. The magnitude of these improvements is outlined in the empirical studies in Sections 3 and 4.

2.2 Partially-factorized variational Bayes with global and local variables

A natural option to improve the mean-field performance is to relax the factorization assumptions on the approximating densities in a way that still allows simple optimization and inference. To accomplish this goal, we consider a partially-factorized representation $\mathcal{Q}_{\text{PFM}} = \{q_{\text{PFM}}(\beta, z) : q_{\text{PFM}}(\beta, z) = q_{\text{PFM}}(\beta | z) \prod_{i=1}^n q_{\text{PFM}}(z_i)\}$ which does not assume independence among the parameters β and the local variables z , thus providing a more flexible family of approximating densities. This new enlarged family \mathcal{Q}_{PFM} allows to incorporate more structure of the actual posterior relative to \mathcal{Q}_{MF} , while retaining tractability. In fact, following Holmes and Held (2006) and recalling that $V = (\nu_p^{-2}I_p + X^T X)^{-1}$, the joint density $p(\beta, z | y)$ under the augmented model (2) can be factorized as $p(\beta, z | y) = p(\beta | z)p(z | y)$, where $p(\beta | z) = \phi_p(\beta - VX^T z; V)$ and $p(z | y) \propto \phi_n(z; I_n + \nu_p^2 XX^T) \prod_{i=1}^n 1[(2y_i - 1)z_i > 0]$ denote the densities of a p -variate Gaussian and an n -variate truncated normal, respectively. The main source of intractability in this factorization of the posterior is the truncated normal density, which requires the evaluation of cumulative distribution functions of n -variate Gaussians with full variance-covariance matrix for inference (Horrace, 2005; Chopin, 2011; Pakman and Paninski, 2014; Botev, 2017; Durante, 2019; Cao et al., 2019). The independence assumption among the augmented data in \mathcal{Q}_{PFM} avoids the intractability of the multivariate truncated normal density $p(z | y)$, while being fully flexible on $q_{\text{PFM}}(\beta | z)$. Crucially, the mean-field solution $q_{\text{MF}}^*(\beta, z)$ belongs to \mathcal{Q}_{PFM} and thus, by minimizing $\text{KL}[q_{\text{PFM}}(\beta, z) || p(\beta, z | y)]$ in \mathcal{Q}_{PFM} , we are guaranteed to obtain improved approximations of the joint posterior density relative to mean-field, as stated in Proposition 1.

Proposition 1 *Let $q_{\text{MF}}^*(\beta, z)$ and $q_{\text{PFM}}^*(\beta, z)$ denote the optimal approximations for $p(\beta, z | y)$ from model (2), under mean-field and partially-factorized variational Bayes, respectively. Then $\text{KL}[q_{\text{PFM}}^*(\beta, z) || p(\beta, z | y)] \leq \text{KL}[q_{\text{MF}}^*(\beta, z) || p(\beta, z | y)]$.*

The above result directly follows from the fact that $q_{\text{MF}}^*(\beta, z)$ belongs to \mathcal{Q}_{PFM} , while $q_{\text{PFM}}^*(\beta, z)$ is the actual minimizer of $\text{KL}[q(\beta, z) || p(\beta, z | y)]$ within the enlarged family \mathcal{Q}_{PFM} . This suggests that our strategy may provide a promising direction to improve quality of posterior approximation. However, to be useful in practice, the solution $q_{\text{PFM}}^*(\beta, z)$ should be simple to derive and the approximate posterior $q_{\text{PFM}}^*(\beta) = \int_{\mathbb{R}^n} q_{\text{PFM}}^*(\beta|z) \prod_{i=1}^n q_{\text{PFM}}^*(z_i) dz = E_{q_{\text{PFM}}^*(z)}[q_{\text{PFM}}^*(\beta | z)]$ of interest should have a tractable form. Theorem 2 and Corollary 1 show that this is possible.

Algorithm 2. Steps of the procedure to obtain $q_{\text{PFM}}^*(\beta, z) = q_{\text{PFM}}^*(\beta | z) \prod_{i=1}^n q_{\text{PFM}}^*(z_i)$

[1] For each $i = 1, \dots, n$, set $\sigma_i^{*2} = (1 - x_i^T V x_i)^{-1}$ and initialize $\bar{z}_i^{(0)} \in \mathfrak{R}$.

[2] **for** t from 1 until convergence of $\text{ELBO}[q_{\text{PFM}}^{(t)}(\beta, z)]$ **do**

for i from 1 to n **do**

 Set $\mu_i^{(t)} = \sigma_i^{*2} x_i^T V X_{-i}^T(\bar{z}_1^{(t)}, \dots, \bar{z}_{i-1}^{(t)}, \bar{z}_{i+1}^{(t-1)}, \dots, \bar{z}_n^{(t-1)})^T$.

 Set $\bar{z}_i^{(t)} = \mu_i^{(t)} + (2y_i - 1)\sigma_i^* \phi(\mu_i^{(t)}/\sigma_i^*) \Phi[(2y_i - 1)\mu_i^{(t)}/\sigma_i^*]^{-1}$.

Output:

$$q_{\text{PFM}}^*(\beta, z) = \phi(\beta - V X^T z; V) \prod_{i=1}^n \phi(z_i - \mu_i^*; \sigma_i^{*2}) \Phi[(2y_i - 1)\mu_i^*/\sigma_i^*]^{-1} 1[(2y_i - 1)z_i > 0].$$

Theorem 2 Under model (2), the KL divergence between $q_{\text{PFM}}(\beta, z) \in \mathcal{Q}_{\text{PFM}}$ and $p(\beta, z | y)$ is minimized at $q_{\text{PFM}}^*(\beta | z) \prod_{i=1}^n q_{\text{PFM}}^*(z_i)$ with

$$q_{\text{PFM}}^*(\beta | z) = p(\beta | z) = \phi_p(\beta - V X^T z; V), \quad V = (\nu_p^{-2} I_p + X^T X)^{-1},$$

$$q_{\text{PFM}}^*(z_i) = \frac{\phi(z_i - \mu_i^*; \sigma_i^{*2})}{\Phi[(2y_i - 1)\mu_i^*/\sigma_i^*]} 1[(2y_i - 1)z_i > 0], \quad \sigma_i^{*2} = (1 - x_i^T V x_i)^{-1}, \quad (i = 1, \dots, n), \quad (8)$$

where $\mu^* = (\mu_1^*, \dots, \mu_n^*)^T$ solves the system $\mu_i^* - \sigma_i^{*2} x_i^T V X_{-i}^T \bar{z}_{-i}^* = 0$, $i = 1, \dots, n$, with X_{-i} denoting the design matrix without the i th row, while \bar{z}_{-i}^* is an $n - 1$ vector obtained by removing the i th element $\bar{z}_i^* = \mu_i^* + (2y_i - 1)\sigma_i^* \phi(\mu_i^*/\sigma_i^*) \Phi[(2y_i - 1)\mu_i^*/\sigma_i^*]^{-1}$, $i = 1, \dots, n$, from the vector $\bar{z}^* = (\bar{z}_1^*, \dots, \bar{z}_n^*)^T$.

In Theorem 2, the new solution for $q_{\text{PFM}}^*(\beta | z)$ follows by noting that $\text{KL}[q_{\text{PFM}}(\beta, z) || p(\beta, z | y)] = \text{KL}[q_{\text{PFM}}(z) || p(z | y)] + E_{q_{\text{PFM}}(z)}\{\text{KL}[q_{\text{PFM}}(\beta | z) || p(\beta | z)]\}$ due to the chain rule for the KL divergence. Therefore, the second summand is 0 if and only if $q_{\text{PFM}}^*(\beta | z) = p(\beta | z)$. The expressions for $q_{\text{PFM}}^*(z_i)$, $i = 1, \dots, n$, are instead a direct consequence of the closure under conditioning property of multivariate truncated Gaussians (Horrace, 2005) which allows to recognize the kernel of a univariate truncated normal in the optimal solution $\exp[E_{q_{\text{PFM}}(z_{-i})}(\log[p(z_i | z_{-i}, y)])]$ (Blei et al., 2017) for $q_{\text{PFM}}^*(z_i)$; see the Supplementary Materials for the detailed proof. Algorithm 2 outlines the steps of the optimization strategy to obtain $q_{\text{PFM}}^*(\beta, z)$. As for classical coordinate ascent variational inference, this routine optimizes the ELBO sequentially with respect to each density $q_{\text{PFM}}(z_i)$, keeping fixed the others at their most recent update, thus producing a strategy that iteratively solves the system of equations for μ^* in Theorem 2 via simple expressions. Indeed, since the form of the approximating densities is already available as in Theorem 2, the steps in Algorithm 2 reduce to update the vector of parameters μ^* via simple functions and matrix operations; see the Supplementary Materials for the expression of $\text{ELBO}[q_{\text{PFM}}(\beta, z)]$.

As stated in Corollary 1, the optimal $q_{\text{PFM}}^*(\beta)$ of interest can be derived from $q_{\text{PFM}}^*(\beta | z)$ and $\prod_{i=1}^n q_{\text{PFM}}^*(z_i)$, and coincides with a tractable SUN density (Arellano-Valle and Azzalini, 2006).

Corollary 1 Let $\bar{Y} = \text{diag}(2y_1 - 1, \dots, 2y_n - 1)$ and $\sigma^* = \text{diag}(\sigma_1^*, \dots, \sigma_n^*)$, then, under (8), the approximate density $q_{\text{PFM}}^*(\beta)$ for β coincides with that of the variable

$$u^{(0)} + V X^T \bar{Y} \sigma^* u^{(1)}, \quad (9)$$

where $u^{(0)} \sim N_p(V X^T \mu^*, V)$, whereas $u^{(1)} = (u_1^{(1)}, \dots, u_n^{(1)})^T$ with $u_i^{(1)} \sim \text{TN}[0, 1, [-(2y_i - 1)\mu_i^*/\sigma_i^*, +\infty]]$, independently for $i = 1, \dots, n$. Equivalently, $q_{\text{PFM}}^*(\beta)$ is the density of the $\text{SUN}_{p,n}(\xi, \Omega, \Delta, \gamma, \Gamma)$ variable with parameters

$$\xi = V X^T \mu^*, \quad \Omega = V + V X^T \sigma^{*2} X V, \quad \Delta = \omega^{-1} V X^T \bar{Y} \sigma^*, \quad \gamma = \bar{Y} \sigma^{*-1} \mu^*, \quad \Gamma = I_n,$$

where ω denotes a $p \times p$ diagonal matrix containing the square roots of the diagonal elements in the covariance matrix Ω , whereas $\bar{\Omega}$ denotes the associated correlation matrix.

The results in Corollary 1 follow by noticing that, under (8), the approximate density for β is the convolution of a p -variate Gaussian and an n -variate truncated normal, thereby producing the density of a SUN (Arellano-Valle and Azzalini, 2006; Azzalini and Capitanio, 2014). This class of random variables generalizes the multivariate Gaussian family via a skewness-inducing mechanism controlled by the matrix Δ which weights the skewing effect produced by an n -variate truncated normal with covariance matrix Γ (Arellano-Valle and Azzalini, 2006; Azzalini and Capitanio, 2014). Besides introducing asymmetric shapes in multivariate Gaussians, the SUN has several closure properties which facilitate inference. However, the evaluation of functionals requires the

Algorithm 3. Strategy to sample from the approximate SUN posterior in Corollary 1

- [1] Draw $u^{(0)} \sim \mathcal{N}_p(VX^T\mu^*, V)$.
- [2] Draw $u_i^{(1)} \sim \text{TN}[0, 1, [-(2y_i - 1)\mu_i^*/\sigma_i^*, +\infty]]$, ($i = 1, \dots, n$), and set $u^{(1)} = (u_1^{(1)}, \dots, u_n^{(1)})^T$.
- [3] Compute $\beta = u^{(0)} + VX^T\bar{Y}\sigma^*u^{(1)}$.

Output: a draw β from the approximate posterior distribution with density $q_{\text{PFM}}^*(\beta)$.

calculation of cumulative distribution functions of n -variate Gaussians (Arellano-Valle and Azzalini, 2006; Azzalini and Capitanio, 2014), which is prohibitive when n is large, unless Γ is diagonal. Recalling Durante (2019), this issue makes Bayesian inference rapidly impractical under the exact posterior $p(\beta | y)$ when n is more than a few hundreds, since $p(\beta | y)$ is a SUN density with non-diagonal Γ_{post} . Instead, the factorized form $\prod_{i=1}^n q_{\text{PFM}}(z_i)$ for $q_{\text{PFM}}(z)$ leads to a SUN approximate density for β in Corollary 1, which crucially relies on a diagonal $\Gamma = I_n$. Such a result allows approximate posterior inference for every n and p via tractable expressions. In particular, recalling the stochastic representation in (9), the first two central moments of β and the predictive distribution are derived in Proposition 2.

Proposition 2 Let $q_{\text{PFM}}^*(\beta)$ be the SUN density in Corollary 1, then

$$\begin{aligned} E_{q_{\text{PFM}}^*(\beta)}(\beta) &= VX^T\bar{z}^*, \\ \text{var}_{q_{\text{PFM}}^*(\beta)}(\beta) &= V + VX^T \text{diag}[\sigma_1^{*2} - (\bar{z}_1^* - \mu_1^*)\bar{z}_1^*, \dots, \sigma_n^{*2} - (\bar{z}_n^* - \mu_n^*)\bar{z}_n^*]XV, \end{aligned} \quad (10)$$

where \bar{z}_i^* , μ_i^* and σ_i^* , $i = 1, \dots, n$ are defined as in Theorem 2. Moreover, the posterior predictive probability $\text{pr}_{\text{PFM}}(y_{\text{NEW}} = 1 | y) = E_{q_{\text{PFM}}^*(\beta)}[\Phi(x_{\text{NEW}}^T\beta)]$ for a new unit with covariates x_{NEW} is

$$\text{pr}_{\text{PFM}}(y_{\text{NEW}} = 1 | y) = E_{q_{\text{PFM}}^*(z)}\{\Phi[x_{\text{NEW}}^T VX^T z(1 + x_{\text{NEW}}^T V x_{\text{NEW}})^{-1/2}]\}, \quad (11)$$

where $q_{\text{PFM}}^*(z)$ can be expressed as the product $\prod_{i=1}^n q_{\text{PFM}}^*(z_i)$ of univariate truncated normal densities $q_{\text{PFM}}^*(z_i) = \phi(z_i - \mu_i^*; \sigma_i^{*2})\Phi[(2y_i - 1)\mu_i^*/\sigma_i^*]^{-1}1[(2y_i - 1)z_i > 0]$, $i = 1, \dots, n$.

Hence, unlike for inference under the exact posterior (Durante, 2019), the calculation of relevant approximate moments such as those in equation (10), only requires the evaluation of cumulative distribution functions of univariate Gaussians. Similarly, the predictive probabilities in equation (11) can be easily evaluated via efficient Monte Carlo methods based on samples from n independent univariate truncated normals with density $q_{\text{PFM}}^*(z_i)$, $i = 1, \dots, n$. Moreover, leveraging (9), samples from the approximate posterior $q_{\text{PFM}}^*(\beta)$ can directly be obtained via a linear combination between realizations from a p -variate Gaussian and from n univariate truncated normals, as shown in Algorithm 3. This strategy allows to study complex approximate functionals of β through simple Monte Carlo methods. If instead the focus is only on $q_{\text{PFM}}^*(\beta_j)$, $j = 1, \dots, p$, one can avoid the cost of simulating from the p -variate Gaussian in Algorithm 3 and just sample from the marginals of $u^{(0)}$ in the additive representation of the SUN to get samples from $q_{\text{PFM}}^*(\beta_j)$ for $j = 1, \dots, p$ at an $\mathcal{O}(pn \cdot \min\{p, n\})$ cost.

We conclude the presentation of our partially-factorized solution by studying its properties in high-dimensional settings as $p \rightarrow \infty$. As discussed in Section 2.1, classical mean-field routines (Consonni and Marin, 2007) yield poor Gaussian approximations of the posterior density in high dimensions, which affect quality of inference and prediction. By relaxing the mean-field assumption we obtain, instead, a skewed approximate density matching the exact posterior for β when $p \rightarrow \infty$, as stated in Theorem 3. We study asymptotic properties under the following assumption.

Assumption 3 Assume that predictors x_{ij} , $i = 1, \dots, n$, $j = 1, \dots, p$, are random variables with $E(x_{ij}) = 0$, $E(x_{ij}^2) = \sigma_x^2$, $E(x_{ij}^4) \leq c_x$ for some $c_x < \infty$ and such that for any $i=1, \dots, n$ and $i' \neq i$: (a) $p^{-1} \sum_{j=1}^p \text{corr}(x_{ij}, x_{i'j}) \rightarrow 0$ as $p \rightarrow \infty$; (b) $p^{-2} \sum_{j=1}^p \sum_{j' \neq j} \text{corr}(x_{ij}^2, x_{i'j'}^2) \rightarrow 0$ as $p \rightarrow \infty$; (c) $p^{-2} \sum_{j=1}^p \sum_{j' \neq j} \text{corr}(x_{ij}x_{i'j}, x_{i'j'}x_{ij'}) \rightarrow 0$ as $p \rightarrow \infty$.

In Assumption 3 we do not require independence among predictors $\{x_{ij}\}$ in the random design, but rather we impose asymptotic conditions on their correlation structure. These conditions are trivially satisfied when predictors are independent and thus Assumption 3 is strictly weaker than Assumption 1 and incorporates the latter. The strongest assumption is arguably 3(a), which requires the average correlation between units to go to 0 as $p \rightarrow \infty$. Note that such assumption does not prevent statistical units from being strongly correlated on a given set of predictors, but rather requires those to be a minority among all predictors, which is a reasonable assumption in large p

scenarios. Conditions 3(b) and 3(c), which deal with correlation across predictors, are arguably much weaker and we expect them to be satisfied in almost any commonly encountered practical scenario. In particular, these conditions allow for pairs of predictors with arbitrarily strong correlation, while requiring the number of such pairs to be $o(p^2)$ as $p \rightarrow \infty$. Also, the empirical results in Sections 3 and 4 suggest that asymptotic exactness of our strategy for large p might hold even beyond the Assumption 3; see e.g. Figure S1 in the Supplementary Materials.

Theorem 3 *Under Assumptions 2–3, we have that $\text{KL}[q_{\text{PFM}}^*(\beta) \parallel p(\beta | y)] \xrightarrow{p} 0$ as $p \rightarrow \infty$, where \xrightarrow{p} denotes convergence in probability.*

Hence, in the high-dimensional settings where current computational strategies are impractical (Chopin and Ridgway, 2017), inference and prediction under the proposed partially-factorized variational approximation is practically feasible, and provides essentially the same results as those obtained under the exact posterior. For instance, Corollary 2 states that, unlike for classical mean-field strategies, our solution is guaranteed to provide increasingly accurate approximations of posterior predictive probabilities as $p \rightarrow \infty$.

Corollary 2 *Let $\text{pr}(y_{\text{NEW}} = 1 | y) = \int \Phi(x_{\text{NEW}}^T \beta) p(\beta | y) d\beta$ denote the exact posterior predictive probability for a new observation with predictors $x_{\text{NEW}} \in \mathfrak{R}^p$. Then, under Assumptions 2–3, we have that $\sup_{x_{\text{NEW}} \in \mathfrak{R}^p} |\text{pr}_{\text{PFM}}(y_{\text{NEW}} = 1 | y) - \text{pr}(y_{\text{NEW}} = 1 | y)| \xrightarrow{p} 0$ as $p \rightarrow \infty$.*

Corollary 2 implies that the error made by the proposed method in approximating the posterior predictive probabilities goes to 0 as $p \rightarrow \infty$, regardless of the choice of $x_{\text{NEW}} \in \mathfrak{R}^p$. On the contrary, since by Theorem 1(c) $\sup_{x_{\text{NEW}} \in \mathfrak{R}^p} |\text{pr}_{\text{MF}}(y_{\text{NEW}} = 1 | y) - \text{pr}(y_{\text{NEW}} = 1 | y)|$ is bounded away from 0 almost surely as $p \rightarrow \infty$, there always exists, for every large p , some x_{NEW} such that the corresponding posterior predictive probability $\text{pr}_{\text{MF}}(y_{\text{NEW}} = 1 | y)$ approximated under classical mean-field variational Bayes does not match the exact one.

Finally, as stated in Theorem 4, the number of iterations required by Algorithm 2 to produce the optimal solution $q_{\text{PFM}}^*(\beta)$ converges to 1 as $p \rightarrow \infty$.

Theorem 4 *Let $q_{\text{PFM}}^{(t)}(\beta)$ be the approximate density for β produced at step (t) by Algorithm 2. Then, under Assumptions 2–3, we have that $\text{KL}[q_{\text{PFM}}^{(1)}(\beta) \parallel p(\beta | y)] \xrightarrow{p} 0$ as $p \rightarrow \infty$.*

According to Theorem 4, Algorithm 2 converges essentially in one iteration as $p \rightarrow \infty$. Thus the computational complexity of the entire routine is provably equal to that of a single iteration of Algorithm 2, which is dominated by an $\mathcal{O}(pn \cdot \min\{p, n\})$ pre-computation cost derived in the Supplementary Materials, where we also highlight how the evaluation of the functionals in Proposition 2 can be achieved at the same cost. More complex functionals of the approximate posterior can be instead obtained at higher costs via Monte Carlo methods based on Algorithm 3.

We shall emphasize that also the computational complexity of approximate inference under mean-field variational Bayes is dominated by the same $\mathcal{O}(pn \cdot \min\{p, n\})$ pre-computation cost. However, as discussed in Sections 2.1–2.2, our partially-factorized solution produces substantially more accurate approximations than classical mean-field. In Sections 3–4, we provide quantitative evidence for these arguments and discuss how the theoretical results in Sections 2.1–2.2 match closely the empirical behavior observed in simulations and applications.

3 Simulation Studies

To illustrate the advantages of the partially-factorized approximation, we provide extensive simulation studies which assess empirical evidence in finite dimension for the asymptotic results in Section 2, and quantify the magnitude of the improvements in scalability and accuracy relative to state-of-the-art competitors. Consistent with these goals and with our main focus on high dimensions, we compare performance against mean-field variational Bayes (Consonni and Marin, 2007), which provides the only widely-implemented alternative strategy, among those discussed in Section 1.1, that can scale to high-dimensional settings as effectively as our method. We refer to Table 1 for further empirical evidence on the computational intractability in high dimensions of other widely-implemented alternatives, such as Hamiltonian Monte Carlo (Hoffman and Gelman, 2014), expectation-propagation (Chopin and Ridgway, 2017), and Monte Carlo inference based on independent and identically distributed samples from the exact posterior (Durante, 2019).

Consistent with the above goals, we consider a scenario in which the data are generated under assumptions compatible with those in Section 2. In particular, we simulate each $y_i \in \{0, 1\}$, for

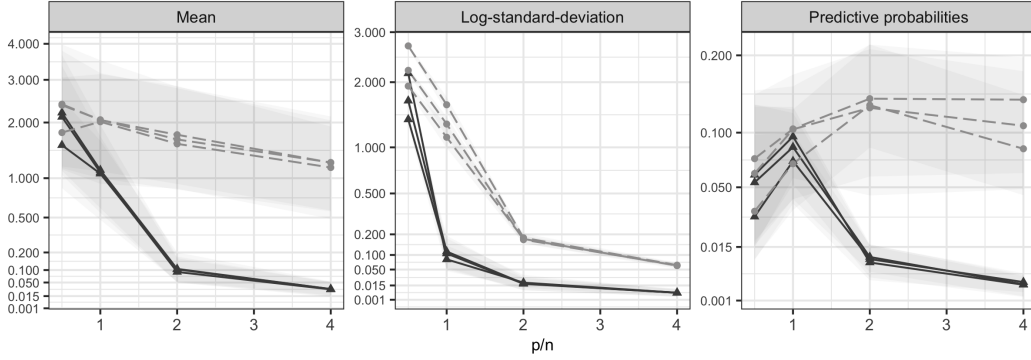


Figure 1: Accuracy in the approximation for three key functionals of the posterior distribution for β . Trajectories for the median of the absolute differences between an accurate but expensive Monte Carlo estimate of such functionals and their approximations provided by partially-factorized variational Bayes (dark grey solid lines) and mean-field variational Bayes (light grey dashed lines), respectively, for increasing values of the ratio p/n , i.e., $p/n \in \{0.5; 1; 2; 4\}$. The different trajectories for each of the two methods correspond to three different settings of the sample size n , i.e., $n \in \{50; 100; 250\}$, whereas the grey areas denote the first and third quartiles computed from the absolute differences. For graphical purposes we consider a square-root scale for the y -axis.

$i = 1, \dots, n$, from the Bernoulli variable $\text{Bern}[\Phi(x_i^T \beta)]$, where $x_i = (1, x_{i2}, \dots, x_{ip})^T$ is a p -dimensional vector of predictors, comprising an intercept term and $p - 1$ covariates simulated from standard normal $N(0, 1)$ variables, independently for $i = 1, \dots, n$ and $j = 2, \dots, p$, and then standardized to have mean 0 and standard deviation 0.5 — as suggested by Gelman et al. (2008) and Chopin and Ridgway (2017). Following the remarks in Gelman et al. (2008), the probit coefficients β_1, \dots, β_p in β are instead simulated from p independent uniforms on the range $[-5, 5]$. To carefully illustrate performance under varying (n, p) settings, we simulate such a dataset under three different sample sizes $n \in \{50; 100; 250\}$ and, for each n , we evaluate performance at varying ratios $p/n \in \{0.5; 1; 2; 4\}$. We emphasize that the dimensions of n and p in these twelve datasets is much low relative to those that can be easily handled under the partially-factorized and mean-field strategies analyzed. In fact, these moderate dimensions are required to make inference still feasible also under the widely-used STAN implementation of Hamiltonian Monte Carlo (Hoffman and Gelman, 2014), which serves here as a benchmark to assess the accuracy of the two variational solutions in approximating key functionals of the exact posterior.

In performing Bayesian inference for the above scenarios, we implement the probit model in (1) under independent weakly informative Gaussian priors with mean 0 and standard deviation 5 for each β_j , $j = 1, \dots, p$ (Gelman et al., 2008; Chopin and Ridgway, 2017). Such priors are then updated with the probit likelihood of the simulated data to obtain a posterior for β in each of the twelve (n, p) settings, which we approximate with both mean-field variational Bayes and our novel partially-factorized solution. Figure 1 illustrates the quality of these two approximations with a focus on three key functionals of the posterior for β , taking as benchmark the Monte Carlo estimates of such functionals computed from 20000 posterior samples of β , under the `rstan` implementation of the Hamiltonian Monte Carlo. The latter strategy leads to accurate estimates of the exact posterior functionals but, as highlighted in Section 1.1 and in Table 1, is clearly impractical in high dimensions. Hence, it is of interest to quantify how far the approximations provided by the two more scalable variational methods are from the STAN Monte Carlo estimates, under different (n, p) settings. In Figure 1, this assessment focuses on the first two posterior moments of each β_j , $j = 1, \dots, p$, and on the out-of-sample predictive probabilities of newly simulated units $i' = 1, \dots, 100$. For such functionals, we represent the median and the quartiles of the absolute differences between the corresponding STAN Monte Carlo estimates and the approximations provided by the two variational methods, at varying combinations of (n, p) . In the first and second panel, the three quartiles are computed on the p absolute differences among the Monte Carlo and approximate estimates for the two posterior moments of each β_j , $j = 1, \dots, p$, respectively, whereas in the third panel these summary measures are computed on the 100 absolute differences for the predictive probabilities of the newly simulated units $i' = 1, \dots, 100$.

According to Figure 1, the partially-factorized solution uniformly improves the accuracy of the mean-field approximation, and the magnitude of such gains increases as p grows relative to n . Notably, the median and the two quartiles of the absolute differences between the STAN estimates and those provided by our novel partially-factorized approximation rapidly shrink toward 0 for all the functionals under analysis, when $p > n$. This means that in such settings the proposed

strategy matches almost perfectly the functionals of interest of the exact posterior, thus providing the same quality in inference and prediction as the one obtained, at massively higher computational costs, under state-of-the-art Hamiltonian Monte Carlo implementations. For instance, while our approximation can be obtained in fractions of seconds in the setting $(n = 250, p = 1000)$, STAN requires several hours, even when considering parallel implementations. On the contrary, the classical mean-field approximation always leads to biased estimates, even when $p > n$, not only for the scales, but also for the locations and the predictive probabilities. As we will clarify in the application in Section 4, such a bias can have dramatic consequences in inference and prediction.

All the above empirical findings are fully coherent with the theoretical results presented in Sections 2.1–2.2 and provide consistent evidence that the behaviors proved in asymptotic regimes are clearly visible even in finite-dimensional $p > n$ settings, without requiring p to be massively higher than n . Also Theorem 4 finds evidence in the simulation study since for all the $p > n$ settings under analysis, Algorithm 2 requires at most 5 iterations to reach convergence, whereas Algorithm 1 needs on average 150 iterations. Finally, the almost perfect overlap in Figure 1 of the trajectories for the different n settings suggests that the quality of the two variational approximations may depend on (p, n) just through the ratio p/n ; see Section 5 for further discussion.

As illustrated in the Supplementary Materials, the above findings apply also to more general data structures which do not meet the assumptions required to prove the theory in Sections 2.1–2.2. These results motivate further exploration in real-world studies, presented in Section 4.

4 High-Dimensional Probit Regression for Alzheimer’s Data

As shown in Chopin and Ridgway (2017), state-of-the-art computational methods for Bayesian binary regression, such as Hamiltonian Monte Carlo (Hoffman and Gelman, 2014), mean-field variational Bayes (Consonni and Marin, 2007) and expectation-propagation (Chopin and Ridgway, 2017) are feasible and powerful procedures in small-to-moderate p settings, but become rapidly impractical or inaccurate in large p contexts, such as $p > 1000$. The overarching focus of the present article is to close this gap and, consistent with this aim, we consider a large p study to quantify the drawbacks encountered by the aforementioned strategies along with the improvements provided by the proposed partially-factorized method in real-world applications.

Following the above remarks, we model presence or absence of Alzheimer’s disease in its early stages as a function of demographic data, genotype and assay results. The original dataset is available in the R library `AppliedPredictiveModeling` and arises from a study of the Washington University to determine if biological measurements from cerebrospinal fluid are useful in modeling and predicting early stages of the Alzheimer’s disease (Craig-Schapiro et al., 2011). In the original article, the authors consider a variety of machine learning procedures to improve the flexibility relative to a basic binary regression model. Here, we avoid excessively complex black-box algorithms and rely on an interpretable probit regression (1), which improves flexibility by simply adding pairwise interactions, thus obtaining $p = 9036$ predictors, including the intercept, collected for 333 individuals. As done for the simulation studies in Section 3, the original measurements have been standardized to have mean 0 and standard deviation 0.5, before entering such variables and their interactions in the probit models (Gelman et al., 2008; Chopin and Ridgway, 2017). Recalling our discussion in Section 3, we recommend to always standardize the predictors and to include the intercept term when implementing the partially-factorized variational approximation in real-world datasets. Besides being a common operation in routine implementations of probit regression (e.g., Gelman et al., 2008; Chopin and Ridgway, 2017), such a standardization typically reduces the correlation between units and thus also between the associated latent variables z_i , making the resulting variational approximation more accurate.

As for the simulation study, we perform Bayesian inference under the above probit model by relying on independent Gaussian priors with mean 0 and standard deviation 5 for each β_j , $j = 1, \dots, 9036$ (Gelman et al., 2008). These priors are updated with the likelihood of $n = 300$

Table 1: Computational time of state-of-the-art routines in the Alzheimer’s application. This includes the running time of the sampling or optimization procedure, and the time to compute means, standard deviations and predictive probabilities, for those routines that were feasible; EP, expectation-propagation; SUN, i.i.d. sampler from the exact SUN posterior; MF-VB, mean-field variational Bayes; PFM-VB, partially-factorized variational Bayes.

	STAN	EP	SUN	MF-VB	PFM-VB
Computational time in minutes	> 360.00	> 360.00	92.27	0.06	0.06

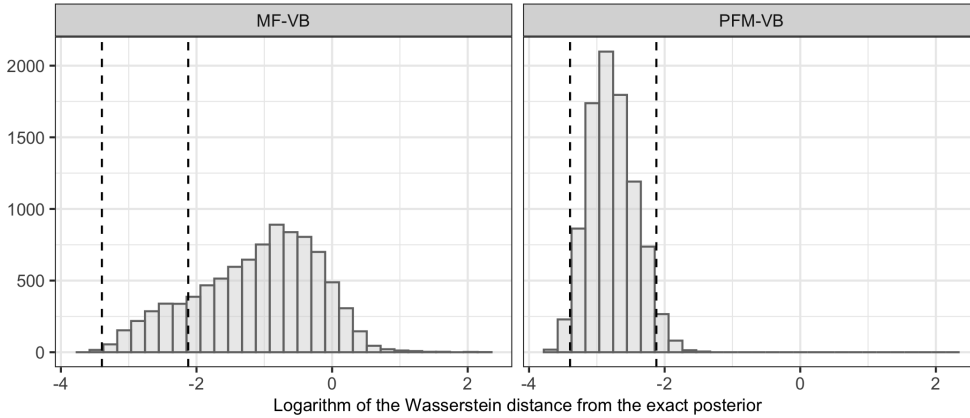


Figure 2: For the two variational approximations, histograms of the log-Wasserstein distances between the $p = 9036$ approximate marginal densities provided by the two variational methods and the exact posterior marginals. These distances are computed leveraging 20000 samples from the approximate and exact marginals. To provide insights on Monte Carlo error, the dashed vertical lines represent the quantiles 2.5% and 97.5% of the log-Wasserstein distances between two different samples of 20000 draws from the same exact posterior marginals. MF-VB, mean-field variational Bayes; PFM-VB, partially-factorized variational Bayes.

units, after holding out 33 individuals to study the behavior of the posterior predictive probabilities in such large p settings, along with the performance of the overall approximation of the posterior. Table 1 provides insights on the computational time of the two variational approximations, and highlights the bottlenecks encountered by relevant routine-use competitors. These include the `rstan` implementation of Hamiltonian Monte Carlo, the expectation-propagation algorithm in the R library `EPGLM`, and the Monte Carlo strategy based on 20000 independent draws from the exact SUN posterior using the algorithm in Durante (2019). As expected, these strategies are impractical in such settings. In particular, `STAN` and expectation-propagation suffer from the large p , whereas sampling from the exact posterior is still feasible, but requires a non-negligible computational effort due to the moderately large n . Variational inference is orders of magnitude faster and, therefore, provides the only viable approach in such settings. These results motivate our main focus on the quality of the two variational approximations in Figures 2–3, taking as a benchmark Monte Carlo inference based on 20000 independent samples from the exact SUN posterior (Durante, 2019). In this example Algorithm 2 requires only 6 iterations to converge, instead of 212 as for Algorithm 1. This result is in line with Theorem 4.

Figure 2 shows the histograms of the log-Wasserstein distances among the $p = 9036$ exact posterior marginals and the associated approximations under the two variational methods. Such quantities are computed with the R function `wasserstein1d`, which uses 20000 values sampled from the approximate and exact marginals. According to these histograms, our partially-factorized solution improves the quality of the mean-field one and, in practice, it matches almost perfectly the exact posterior since it provides distances within the range of values obtained by comparing two different samples of 20000 draws from the same exact posterior marginals. Hence, most of the variability in the partially-factorized approximation is arguably due to Monte Carlo error. This high accuracy is achieved despite the presence of 5000 pairs of predictors with a correlation above 0.85, thus confirming the high quality of our new solution in realistic settings.

Consistent with Theorem 1, the low quality of the classical mean-field solution is mostly due to a tendency to over-shrink towards 0 the locations of the actual posterior. This behavior is displayed in the first panel of Figure 3, which compares the posterior expectations computed from 20000 values sampled from the exact SUN posterior with those provided by the closed-form expressions under the two variational approximations reported in Section 2. Also the standard deviations are slightly under-estimated relative to our novel approximation, that notably removes bias also in the second order moments. Consistent with the results in Figure 2, the slight variability of the estimates provided by our solution in the second panel of Figure 3 is arguably due to Monte Carlo error. In Figure 3, we also assess the quality in the approximation of the exact posterior predictive probabilities for the 33 held-out individuals. These measures are fundamental for prediction and, unlike for the first two marginal moments, their evaluation depends on the behavior of the entire posterior since it relies on a non-linear mapping of a linear combination of the parameters β . In the third panel of Figure 3, the proposed approximation essentially matches the exact posterior predictive probabilities, thus providing reliable classification and uncertainty quantifi-

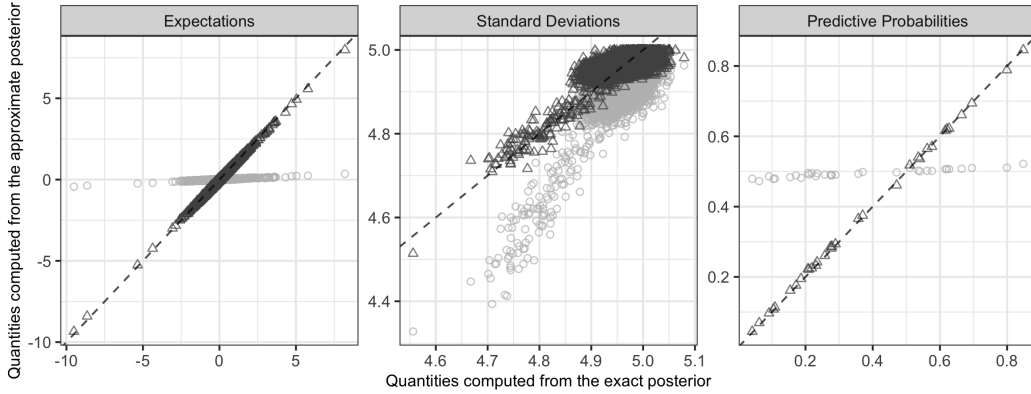


Figure 3: Scatterplots comparing the posterior expectations, standard deviations and predictive probabilities computed from 20000 values sampled from the exact SUN posterior, with those provided by the mean-field variational Bayes (light grey circles) and partially-factorized variational Bayes (dark grey triangles).

cation. Instead, as expected from the theoretical results in Theorem 1, mean-field over-shrinks these quantities towards 0.5. This leads to a test deviance $-\sum_{i=1}^{33} \{y_{i,\text{NEW}} \log \hat{\text{pr}}_{\text{MF}}(y_{i,\text{NEW}} = 1 | y) + (1 - y_{i,\text{NEW}}) \log [1 - \hat{\text{pr}}_{\text{MF}}(y_{i,\text{NEW}} = 1 | y)]\}$ for mean-field variational Bayes of 22.31, dramatically increasing the test deviance of 14.62 under the proposed partially-factorized solution. The latter is, instead, in line with the test deviance of 14.58 obtained via Monte Carlo using independent samples from the exact SUN posterior. As clarified with additional applications to other medical datasets in the Supplementary Materials, the low-quality approximations of mean-field can have a serious impact on predictive performance, whereas the partially-factorized approximation still preserves accuracy. In the Supplementary Materials we also provide further results for the Alzheimer’s study and replicate the analyses by setting a prior variance of order $\mathcal{O}(1/p)$ to induce shrinkage in high dimension. As a consequence of this strong shrinkage effect also the exact posterior means increasingly shrink towards 0, thus mitigating the issues of classical mean-field approximations which, however, still maintain a bias that is not present under the proposed partially-factorized solution, in all settings.

5 Discussion

While our contribution provides an important advancement in a non-Gaussian regression context where previously available Bayesian computational strategies are unsatisfactory (Chopin and Ridgway, 2017), the results in this article open new avenues for future research. For instance, the theory on mean-field approximations and mode estimators presented in Section 2.1 for large p settings points to the need of further theoretical studies on the use of such quantities in high-dimensional regression with non-Gaussian responses. In these contexts, our idea of relying on a partially-factorized approximating family could provide a general strategy to solve potential issues of current global-local approximations; see Cao et al. (2020) and Fasano and Durante (2020) for ongoing research in this direction that has been motivated by the ideas and methods developed in this article. We shall also emphasize that, although our focus on Gaussian priors with variance possibly decreasing with p already allows to enforce shrinkage in high dimensions, such a setting also provides a relevant building-block which can be included in more complex scale mixtures of Gaussian priors to obtain improved theoretical and practical performance in state-of-the-art approximations under sparse settings. Finally, it would be of interest to extend the asymptotic results in Theorems 1, 3 and 4 to settings in which n grows with p at some rate. Motivated by the results in Figure 1, we conjecture that n growing sublinearly with p is a sufficient condition to obtain asymptotic-exactness results analogous to Theorem 3.

Acknowledgements

Daniele Durante is also affiliated to the Bocconi Institute for Data Science and Analytics (BIDSA) at Bocconi University, Milan, and acknowledges the support from MIUR–PRIN 2017 project 20177BR–JXS. Giacomo Zanella is affiliated to the Innocenzo Gasparini Institute for Economic Research (IGIER) and the Bocconi Institute for Data Science and Analytics (BIDSA) at Bocconi University, Milan, and acknowledges the support from MIUR–PRIN project 2015SNS29B.

Supplementary Materials

A ELBO and cost of partially-factorized variational Bayes

We discuss the computational cost of partially-factorized variational Bayes, showing that the whole routine requires matrix pre-computations with $\mathcal{O}(pn \cdot \min\{p, n\})$ cost and iterations with $\mathcal{O}(n \cdot \min\{p, n\})$ cost. Consider first Algorithm 2. When $p \geq n$, one can pre-compute XVX^\top at $\mathcal{O}(pn^2)$ cost by applying the Woodbury's identity to V , and then perform each iteration at $\mathcal{O}(n^2)$ cost. Instead, when $p < n$, one can pre-compute XV at $\mathcal{O}(p^2n)$ cost, and then perform each iteration at $\mathcal{O}(pn)$ cost noting that

$$\mu_i^{(t)} = \sigma_i^{*2} \sum_{j=1}^p (XV)_{ij} \alpha_j^{(t,i)}, \quad \text{with } \alpha_j^{(t,i)} = \sum_{i'=1}^{i-1} x_{i'j} \bar{z}_{i'}^{(t)} + \sum_{i'=i+1}^n x_{i'j} \bar{z}_{i'}^{(t-1)},$$

where the vector $\alpha^{(t,i)} = (\alpha_1^{(t,i)}, \dots, \alpha_p^{(t,i)})^\top$ can be computed at $\mathcal{O}(p)$ cost from $\alpha^{(t,i-1)}$ exploiting the recursive equations

$$\alpha_j^{(t,i)} = \alpha_j^{(t,i-1)} - x_{ij} \bar{z}_i^{(t-1)} + x_{i-1,j} \bar{z}_{i-1}^{(t)}.$$

Hence, computing $\mu_i^{(t)}$ for $i = 1, \dots, n$, which is the most expensive part of Algorithm 2, can be done in $\mathcal{O}(np)$ operations using XV and $\alpha^{(t,i)}$. With simple calculations one can check that also computing the ELBO requires $\mathcal{O}(n \cdot \min\{p, n\})$ operations, as it involves quadratic forms of $n \times n$ matrices with rank at most $\min\{p, n\}$. Indeed, calling $\Lambda = (I_n + \nu_p^2 X X^\top)^{-1}$, it holds

$$\begin{aligned} \text{ELBO}[q_{\text{PFM}}^{(t)}(\beta, z)] &= \text{ELBO}[q_{\text{PFM}}^{(t)}(z)] = E_{q_{\text{PFM}}^{(t)}(z)}[\log p(z, y)] - E_{q_{\text{PFM}}^{(t)}(z)}[\log q(z)] \\ &= \text{const} + \sum_{i=1}^n \log \Phi[(2y_i - 1)\mu_i^{(t)}/\sigma_i^*] + 0.5 E_{q_{\text{PFM}}^{(t)}(z)}[(z - \mu^{(t)})^\top \sigma^{*-1} (z - \mu^{(t)}) - z^\top \Lambda z] \\ &= \text{const} - 0.5 \sum_{i=1}^n \{ \Lambda_{ii} E_{q_{\text{PFM}}^{(t)}(z_i)}(z_i^2) - 2 \log \Phi[(2y_i - 1)\mu_i^{(t)}/\sigma_i^*] - E_{q_{\text{PFM}}^{(t)}(z_i)}(z_i^2)/\sigma_i^{*2} \\ &\quad + 2 \bar{z}_i^{(t)} \mu_i^{(t)}/\sigma_i^{*2} - (\mu_i^{(t)}/\sigma_i^*)^2 \} - \sum_{i>j} \Lambda_{ij} \bar{z}_i^{(t)} \bar{z}_j^{(t)}, \end{aligned}$$

with $E_{q_{\text{PFM}}^{(t)}(z_i)}(z_i^2) = \mu_i^{(t)2} + \sigma_i^{*2} + (2y_i - 1)\mu_i^{(t)} \sigma_i^* \phi(\mu_i^{(t)}/\sigma_i^*) \Phi[(2y_i - 1)\mu_i^{(t)}/\sigma_i^*]^{-1}$, and $\bar{z}_i^{(t)}$ defined as in Algorithm 2.

Given the output of Algorithm 2, the mean of β under the partially-factorized approximation can be computed at $\mathcal{O}(pn \cdot \min\{p, n\})$ cost noting that, by (10), $E_{q_{\text{PFM}}^*(\beta)}(\beta) = VX^\top \bar{z}^*$ and that VX^\top can be computed at $\mathcal{O}(pn \cdot \min\{p, n\})$ cost using either its definition, when $p \leq n$, or the equality $VX^\top = \nu_p^2 X^\top (I_n + \nu_p^2 X X^\top)^{-1}$, when $p > n$. Given VX^\top , one can compute the covariance matrix of β under partially-factorized variational Bayes at $\mathcal{O}(p^2n)$ cost using (10), and applying Woodbury's identity to V when $p > n$. On the other hand, the marginal variances $\text{var}_{q_{\text{PFM}}^*(\beta_j)}(\beta_j)$, $j = 1, \dots, p$, can be obtained at $\mathcal{O}(pn \cdot \min\{p, n\})$ cost by first computing VX^\top , and then exploiting (10) along with $V_{jj} = \nu_p^2 [1 - \sum_{i=1}^n (VX^\top)_{ji} x_{ij}]$, which follows from $V(I_p + \nu_p^2 X^\top X) = \nu_p^2 I_p$.

Finally, the Monte Carlo estimates of the approximate predictive probabilities $\text{pr}_{\text{PFM}}(y_{\text{NEW}} = 1 \mid y)$ in (11) can be computed at $\mathcal{O}(pn \cdot \min\{p, n\} + nR)$ cost, where R denotes the number of Monte Carlo samples. Indeed, simulating i.i.d. realizations $z^{(r)}$, $r = 1, \dots, R$, from $q_{\text{PFM}}^*(z)$ has an $\mathcal{O}(nR)$ cost, while computing $\Phi[x_{\text{NEW}}^\top VX^\top z^{(r)} (1 + x_{\text{NEW}}^\top V x_{\text{NEW}})^{-1/2}]$ for $r = 1, \dots, R$ has $\mathcal{O}(pn \cdot \min\{p, n\} + nR)$ cost because, given VX^\top , the computation of $x_{\text{NEW}}^\top VX^\top z^{(r)}$ for $r = 1, \dots, R$ requires $\mathcal{O}(pn + nR)$ operations, while the computation of $x_{\text{NEW}}^\top V x_{\text{NEW}}$ can be done in $\mathcal{O}(pn \cdot \min\{p, n\})$ operations using either its original definition, when $p \leq n$, or Woodbury's identity on V , when $p > n$, leading to $x_{\text{NEW}}^\top V x_{\text{NEW}} = \nu_p^2 [\|x_{\text{NEW}}\|^2 - \nu_p^2 (X x_{\text{NEW}})^\top (I_n + \nu_p^2 X X^\top)^{-1} (X x_{\text{NEW}})]$.

B Proofs of Propositions, Lemmas, Theorems and Corollaries

We first prove some general lemmas that will be useful for the proofs of Theorems 1, 3 and 4. We use the notation $M = o(p^d)$ for a matrix M to indicate that all the entries of M are $o(p^d)$ as $p \rightarrow \infty$. Almost sure convergence and convergence in probability are denoted, respectively, by $\xrightarrow{\text{a.s.}}$ and \xrightarrow{p} . Moreover, convergence of matrices, both almost sure and in probability, is intended element-wise.

Lemma 1 *Let $(w_j)_{j \geq 1}$ be a sequence of independent random variables with mean 0 and variance bounded over j . Then $p^{-1/2-\delta} \sum_{j=1}^p w_j \xrightarrow{\text{a.s.}} 0$ as $p \rightarrow \infty$ for every $\delta > 0$.*

Lemma 1 is a variant of the strong law of large numbers and it follows from Khintchine–Kolmogorov convergence theorem and Kronecker’s lemma. Being a classical result, we omit the proof for brevity.

Lemma 2 *Under Assumptions 1–2, for every $\delta > 0$ we have that $(\sigma_x^2 p)^{-1} X X^\top \stackrel{a.s.}{\rightarrow} I_n + o(p^{-1/2+\delta})$ and $(1 + \sigma_x^2 p \nu_p^2)^{-1} (I_n + \nu_p^2 X X^\top) \stackrel{a.s.}{\rightarrow} I_n$ as $p \rightarrow \infty$. Under Assumptions 2 and 3, we have that $(\sigma_x^2 p)^{-1} X X^\top \xrightarrow{p} I_n$ and, consequently, $(1 + \sigma_x^2 p \nu_p^2)^{-1} (I_n + \nu_p^2 X X^\top) \xrightarrow{p} I_n$ as $p \rightarrow \infty$.*

Proof. Considering the first part of the statement, by Assumption 1, $(x_{ij}^2)_{j \geq 1}$ are independent random variables with mean σ_x^2 and variance bounded over j . Thus

$$p^{1/2-\delta} [(\sigma_x^2 p)^{-1} X X^\top - I_n]_{ii} = p^{-1/2-\delta} \sum_{j=1}^p (\sigma_x^{-2} x_{ij}^2 - 1) \stackrel{a.s.}{\rightarrow} 0$$

as $p \rightarrow \infty$ by Lemma 1. Similarly, when $i \neq i'$, $(x_{ij} x_{i'j})_{j \geq 1}$ are independent variables with mean 0 and variance $\sigma_x^4 < \infty$. Hence

$$p^{1/2-\delta} [(\sigma_x^2 p)^{-1} X X^\top - I_n]_{i i'} = \sigma_x^{-2} p^{-1/2-\delta} \sum_{j=1}^p x_{ij} x_{i'j} \stackrel{a.s.}{\rightarrow} 0$$

as $p \rightarrow \infty$ by Lemma 1. It follows that $(\sigma_x^2 p)^{-1} X X^\top \stackrel{a.s.}{\rightarrow} I_n + o(p^{-1/2+\delta})$ as $p \rightarrow \infty$. Finally, since by Assumption 2, $p \nu_p^2$ converges to a positive constant or to infinity, in both cases we have

$$\begin{aligned} & (1 + \sigma_x^2 p \nu_p^2)^{-1} (I_n + \nu_p^2 X X^\top) \\ &= (1 + \sigma_x^2 p \nu_p^2)^{-1} I_n + (1 + \sigma_x^2 p \nu_p^2)^{-1} (\sigma_x^2 p \nu_p^2) (\sigma_x^2 p)^{-1} X X^\top \stackrel{a.s.}{\rightarrow} I_n, \quad \text{as } p \rightarrow \infty. \end{aligned} \quad (12)$$

Consider now the second part of the statement. Since $[(\sigma_x^2 p)^{-1} X X^\top]_{ii} = p^{-1} \sum_{j=1}^p \sigma_x^{-2} x_{ij}^2$ and $E(\sigma_x^{-2} x_{ij}^2) = 1$ for any $j = 1, \dots, p$, Chebyshev’s inequality implies that, for any $\epsilon > 0$,

$$\begin{aligned} & \text{pr}[|p^{-1} \sum_{j=1}^p \sigma_x^{-2} x_{ij}^2 - 1| > \epsilon] \\ & \leq (p^2 \epsilon^2)^{-1} \text{var}(\sum_{j=1}^p \sigma_x^{-2} x_{ij}^2) = (\epsilon p^2 \sigma_x^4)^{-1} [\sum_{j=1}^p \text{var}(x_{ij}^2) + \sum_{j=1}^p \sum_{j' \neq j} \text{cov}(x_{ij}^2, x_{i'j'}^2)] \\ & \leq (\epsilon p \sigma_x^4)^{-1} (\max_{j=1, \dots, p} \{E(x_{ij}^4)\} - 1) + (\epsilon p^2 \sigma_x^2)^{-1} \sum_{j=1}^p \sum_{j' \neq j} \text{corr}(x_{ij}^2, x_{i'j'}^2) \rightarrow 0, \end{aligned}$$

as $p \rightarrow \infty$, by Assumption 3(b) and $\sup_{j \geq 1} \{E(x_{ij}^4)\} < \infty$. Thus $[(\sigma_x^2 p)^{-1} X X^\top]_{ii} \xrightarrow{p} 1$ as $p \rightarrow \infty$ for any $i = 1, \dots, n$.

We now consider the off-diagonal and show $[(\sigma_x^2 p)^{-1} X X^\top]_{i i'} = p^{-1} \sum_{j=1}^p \sigma_x^{-2} x_{ij} x_{i'j} \xrightarrow{L^2} 0$ as $p \rightarrow \infty$ for any $i' \neq i$, which implies the desired result. Indeed,

$$E[(p^{-1} \sum_{j=1}^p \sigma_x^{-2} x_{ij} x_{i'j})^2] = \text{var}(p^{-1} \sum_{j=1}^p \sigma_x^{-2} x_{ij} x_{i'j}) + [E(p^{-1} \sum_{j=1}^p \sigma_x^{-2} x_{ij} x_{i'j})]^2.$$

By the Cauchy–Schwarz inequality we have

$$\begin{aligned} & \text{var}(p^{-1} \sum_{j=1}^p \sigma_x^{-2} x_{ij} x_{i'j}) \\ &= (p \sigma_x^2)^{-2} \sum_{j=1}^p \text{var}(x_{ij} x_{i'j}) + (p \sigma_x)^{-2} \sum_{j=1}^p \sum_{j' \neq j} \text{corr}(x_{ij} x_{i'j}, x_{i'j'} x_{i j'}) \\ &\leq (p \sigma_x^2)^{-2} \sum_{j=1}^p [E(x_{ij}^4) E(x_{i'j}^4)]^{1/2} + (p \sigma_x)^{-2} \sum_{j=1}^p \sum_{j' \neq j} \text{corr}(x_{ij} x_{i'j}, x_{i'j'} x_{i j'}) \rightarrow 0 \end{aligned}$$

as $p \rightarrow \infty$ by Assumption 3(c) and $\sup_{i=1, \dots, n; j \geq 1} \{E(x_{ij}^4)\} < \infty$. Moreover

$$E(p^{-1} \sum_{j=1}^p \sigma_x^{-2} x_{ij} x_{i'j}) = p^{-1} \sum_{j=1}^p \text{corr}(x_{ij}, x_{i'j}) \rightarrow 0$$

as $p \rightarrow \infty$ by Assumption 3(a). The above derivations imply $[(\sigma_x^2 p)^{-1} X X^\top]_{i i'} \xrightarrow{L^2} 0$, from which it follows $[(\sigma_x^2 p)^{-1} X X^\top]_{i i'} \xrightarrow{p} 0$ as $p \rightarrow \infty$. Finally, calculations analogous to (12) imply $(1 + \sigma_x^2 p \nu_p^2)^{-1} (I_n + \nu_p^2 X X^\top) \xrightarrow{p} I_n$ as $p \rightarrow \infty$. \square

Lemma 3 *Set $H = X V X^\top$. Then, under Assumptions 1–2, we have that $(1 + \sigma_x^2 p \nu_p^2) (I_n - H) \stackrel{a.s.}{\rightarrow} I_n$ as $p \rightarrow \infty$. In particular, for $p \rightarrow \infty$, we have that $H \stackrel{a.s.}{\rightarrow} [(\alpha \sigma_x^2) / (1 + \alpha \sigma_x^2)] I_n$, where $(\alpha \sigma_x^2) / (1 + \alpha \sigma_x^2) = 1$ if $\alpha = \infty$. Under Assumptions 2–3, the same holds, with a.s. convergence replaced by convergence in probability.*

Proof. Applying Woodbury identity to $(I_n + \nu_p^2 X X^\top)^{-1}$ and using $V = (\nu_p^{-2} I_p + X^\top X)^{-1}$, we have

$$\begin{aligned} (I_n + \nu_p^2 X X^\top)^{-1} &= I_n - \nu_p^2 X (I_p + \nu_p^2 X^\top X)^{-1} X^\top \\ &= I_n - X (\nu_p^{-2} I_p + X^\top X)^{-1} X^\top = I_n - H. \end{aligned} \quad (13)$$

Thus, under Assumptions 1 and 2,

$$[(1 + \sigma_x^2 p \nu_p^2)(I_n - H)]^{-1} = (1 + \sigma_x^2 p \nu_p^2)^{-1} (I_n + \nu_p^2 X X^\top) \xrightarrow{\text{a.s.}} I_n$$

as $p \rightarrow \infty$ by Lemma 2. Under Assumptions 2 and 3 the same convergence holds in probability again by Lemma 2. The convergence of $(1 + \sigma_x^2 p \nu_p^2)(I_n - H)$ to I_n follows by the one of $[(1 + \sigma_x^2 p \nu_p^2)(I_n - H)]^{-1}$ and the continuity of the inverse operator over the set of non-singular $n \times n$ matrices.

Finally, to obtain the convergence of H , note that by (13) we have

$$H = I_n - (1 + \sigma_x^2 p \nu_p^2)^{-1} (1 + \sigma_x^2 p \nu_p^2) (I_n + \nu_p^2 X X^\top)^{-1}. \quad (14)$$

By Lemma 2 and the above mentioned continuity of the inverse operator, under Assumptions 1 and 2, $(1 + \sigma_x^2 p \nu_p^2)(I_n + \nu_p^2 X X^\top)^{-1} \xrightarrow{\text{a.s.}} I_n$ as $p \rightarrow \infty$. Thus, if $\alpha = \lim_{p \rightarrow \infty} p \nu_p^2 = \infty$, $H \xrightarrow{\text{a.s.}} I_n$ as $p \rightarrow \infty$, since the second addend in (14) converges a.s. to the null matrix. On the other hand, if $\alpha = \lim_{p \rightarrow \infty} p \nu_p^2 < \infty$, the second addend converges a.s. to $(1 + \alpha \sigma_x^2)^{-1} I_n$ as $p \rightarrow \infty$, and thus we have that, for $p \rightarrow \infty$,

$$H \xrightarrow{\text{a.s.}} I_n - (1 + \alpha \sigma_x^2)^{-1} I_n = [\alpha \sigma_x^2 / (1 + \alpha \sigma_x^2)] I_n,$$

as desired. Under Assumptions 2 and 3, the same argument holds, replacing a.s. convergence with convergence in probability. \square

Lemma 4 *Let $\mu_l^{(p)} \rightarrow 0$ and $\Sigma_l^{(p)} \rightarrow I_n$ as $p \rightarrow \infty$ for $l = 1, 2$, with $\mu_l^{(p)} \in \mathfrak{R}^n$ and $\Sigma_l^{(p)} \in \mathfrak{R}^{n^2}$, $l = 1, 2$. Then $\text{KL}[\text{TN}(\mu_1^{(p)}, \Sigma_1^{(p)}, \mathbb{A}) \parallel \text{TN}(\mu_2^{(p)}, \Sigma_2^{(p)}, \mathbb{A})] \rightarrow 0$ as $p \rightarrow \infty$, with \mathbb{A} denoting an orthant of \mathfrak{R}^n that, in the rest of the derivations, is defined as $\mathbb{A} = \{z \in \mathfrak{R}^n: (2y_i - 1)z_i > 0\}$.*

Proof. By definition, $\text{KL}[\text{TN}(\mu_1^{(p)}, \Sigma_1^{(p)}, \mathbb{A}) \parallel \text{TN}(\mu_2^{(p)}, \Sigma_2^{(p)}, \mathbb{A})]$ is equal to

$$\log[(\psi_1^{(p)})^{-1} \psi_2^{(p)}] + \frac{1}{2} \log[\det(\Sigma_1^{(p)})^{-1} \det(\Sigma_2^{(p)})] + (\psi_1^{(p)} 2\pi)^{-n/2} \det(\Sigma_1^{(p)})^{-1/2} \int_{\mathbb{A}} f_p(u) du,$$

where $\psi_l^{(p)} = \text{pr}(u_l^{(p)} \in \mathbb{A})$ with $u_l^{(p)} \sim \text{N}_n(\mu_l^{(p)}, \Sigma_l^{(p)})$, for $l = 1, 2$, and

$$\begin{aligned} f_p(u) &= g_p(u) \exp[-0.5(u - \mu_1^{(p)})^\top (\Sigma_1^{(p)})^{-1} (u - \mu_1^{(p)})], \quad \text{with} \\ g_p(u) &= -0.5[(u - \mu_1^{(p)})^\top (\Sigma_1^{(p)})^{-1} (u - \mu_1^{(p)}) - (u - \mu_2^{(p)})^\top (\Sigma_2^{(p)})^{-1} (u - \mu_2^{(p)})]. \end{aligned}$$

Since $\mu_l^{(p)} \rightarrow 0$ and $\Sigma_l^{(p)} \rightarrow I_n$ as $p \rightarrow \infty$, we have that $\text{N}_n(\mu_l^{(p)}, \Sigma_l^{(p)}) \rightarrow \text{N}_n(0, I_n)$ in distribution and $\psi_l^{(p)} \rightarrow 2^{-n}$ by the Portmanteau theorem, thereby implying $\log[(\psi_1^{(p)})^{-1} \psi_2^{(p)}] \rightarrow 0$.

Moreover, by the continuity of $\det(\cdot)$, it also follows that $\det(\Sigma_l^{(p)}) \rightarrow \det(I_n) = 1$ as $p \rightarrow \infty$, and, therefore,

$$\log[\det(\Sigma_1^{(p)})^{-1} \det(\Sigma_2^{(p)})] \rightarrow 0 \text{ as } p \rightarrow \infty.$$

Moreover, $\Sigma_l^{(p)} \rightarrow I_n$ implies that all the eigenvalues of $\Sigma_l^{(p)}$ converge to 1 as $p \rightarrow \infty$ for $l = 1, 2$, and thus are eventually bounded away from 0 and ∞ . Therefore, there exist positive, finite constants m, M and k such that

$$m \|u - \mu_l^{(p)}\|^2 \leq (u - \mu_l^{(p)})^\top (\Sigma_l^{(p)})^{-1} (u - \mu_l^{(p)}) \leq M \|u - \mu_l^{(p)}\|^2, \text{ for } l = 1, 2 \text{ and } p \geq k.$$

Calling $b = \sup_{p \geq 1, l \in \{1, 2\}} \|\mu_l^{(p)}\| < \infty$, and using standard properties of norms, we have

$$m(\|u\|^2 - 2b\|u\|) \leq (u - \mu_l^{(p)})^\top (\Sigma_l^{(p)})^{-1} (u - \mu_l^{(p)}) \leq (M\|u\|^2 + Mb), \text{ for } l = 1, 2 \text{ and } p \geq k,$$

from which we obtain that, for $p \geq k$, $|f_p(u)| \leq (M\|u\|^2 + Mb) \exp(-m\|u\|^2/2 + b\|u\|)$, where the latter is an integrable function on \mathfrak{R}^n . Therefore we can apply the dominated convergence theorem and obtain $\lim_{p \rightarrow \infty} \int_{\mathbb{A}} f_p(u) du = \int_{\mathbb{A}} \lim_{p \rightarrow \infty} f_p(u) du = 0$ as desired. \square

B.1 Proof of Theorem 1

Let $\bar{\beta}^* = \arg \max_{\beta \in \mathfrak{R}^p} \ell(\beta)$, where $\ell(\beta) = -(2\nu_p^2)^{-1} \|\beta\|^2 + \sum_{i=1}^n \log \Phi[(2y_i - 1)x_i^\top \beta]$ denotes the log-posterior up to an additive constant under (1). Note that $\bar{\beta}^*$ is unique because $\ell(\beta)$ is strictly concave (Haberman, 1974).

Lemma 5 Under Assumption 1, we have $\nu_p^{-1} \|\bar{\beta}^*\| \xrightarrow{a.s.} 0$ as $p \rightarrow \infty$.

Proof. Since $\log \Phi[(2y_i - 1)x_i^\top \beta] < 0$ for any $i = 1, \dots, n$, we have $\ell(\beta) < -(2\nu_p^2)^{-1} \|\beta\|^2$ and thus $\nu_p^{-2} \|\beta\|^2 < -0.5\ell(\beta)$ for any $\beta \in \mathfrak{R}^p$. Thus, It follows that $\nu_p^{-2} \|\bar{\beta}^*\|^2 < -0.5\ell(\bar{\beta}^*) = -0.5 \sup_{\beta \in \mathfrak{R}^p} \ell(\beta)$.

We now prove that $\sup_{\beta \in \mathfrak{R}^p} \ell(\beta) \xrightarrow{a.s.} 0$ as $p \rightarrow \infty$. Define $\tilde{\beta} = (\tilde{\beta}_j)_{j=1}^p \in \mathfrak{R}^p$ as

$$\tilde{\beta}_j = p^{-2/3} (2y_{\lceil nj/p \rceil} - 1) x_{\lceil nj/p \rceil, j}, \quad j = 1, \dots, p,$$

where $\lceil a \rceil$ denotes the smallest integer larger or equal to a . It follows that

$$p^{-1/3} x_i^\top \tilde{\beta} = p^{-1} (2y_i - 1) \sum_{j \in D_i} x_{ij}^2 + p^{-1} \sum_{j \notin D_i} \zeta_{ij},$$

where $D_i = \{j \in \{1, \dots, p\} : (i-1)p/n < j \leq ip/n\}$ and $\zeta_{ij} = x_{ij} x_{\lceil nj/p \rceil, j} (2y_{\lceil nj/p \rceil} - 1)$. Now, note that the $(x_{ij}^2)_{j \in D_i}$ and $(\zeta_{ij})_{j \notin D_i}$ are independent variables with bounded variance, the size of each D_i is asymptotic to $n^{-1}p$ as $p \rightarrow \infty$ and $E(\zeta_{ij}) = 0$ for $j \notin D_i$. Hence, Lemma 1 implies that $\lim_{p \rightarrow \infty} p^{-1/3} x_i^\top \tilde{\beta} \stackrel{a.s.}{=} n^{-1} (2y_i - 1) \sigma_x^2$. Assuming $\sigma_x^2 > 0$ without loss of generality — when $\sigma_x^2 = 0$ it holds $\bar{\beta}^* \stackrel{a.s.}{=} 0$ — it follows that $x_i^\top \tilde{\beta} \stackrel{a.s.}{\rightarrow} +\infty$ if $y_i = 1$ and $x_i^\top \tilde{\beta} \stackrel{a.s.}{\rightarrow} -\infty$ if $y_i = 0$ as $p \rightarrow \infty$ and therefore $\sum_{i=1}^n \log \Phi[(2y_i - 1)x_i^\top \tilde{\beta}] \xrightarrow{a.s.} 0$ as $p \rightarrow \infty$. Moreover, $\|\tilde{\beta}\|^2 = p^{-1/3} (p^{-1} \sum_{j=1}^p x_{\lceil nj/p \rceil, j}^2) \xrightarrow{a.s.} 0$ as $p \rightarrow \infty$ by Lemma 1. Thus $0 \geq \sup_{\beta \in \mathfrak{R}^p} \ell(\beta) \geq \ell(\tilde{\beta}) \xrightarrow{a.s.} 0$ as $p \rightarrow \infty$ as desired. \square

Lemma 6 Let q_1 and q_2 be probability distributions on \mathfrak{R}^p . Then, for any $x_{\text{NEW}} \in \mathfrak{R}^p$, we have $\text{KL}[q_1 \parallel q_2] \geq 2 |\text{pr}_{q_1} - \text{pr}_{q_2}|^2$, where $\text{pr}_{q_l} = \int \Phi(x_{\text{NEW}}^\top \beta) q_l(\beta) d\beta$ for $l = 1, 2$.

Proof. By Pinsker's inequality we have that, $\text{KL}[q_1 \parallel q_2] \geq 2 \text{TV}[q_1, q_2]^2$ where $\text{TV}[\cdot, \cdot]$ denotes the total variation distance between probability distributions. Recall also that $\text{TV}[q_1, q_2] = \sup_{h: \mathfrak{R}^p \rightarrow [0, 1]} |\int_{\mathfrak{R}^p} h(\beta) q_1(\beta) d\beta - \int_{\mathfrak{R}^p} h(\beta) q_2(\beta) d\beta|$. Taking $h(\beta) = \Phi(x_{\text{NEW}}^\top \beta)$ we obtain the desired statement. \square

Proof of Theorem 1 As noted in Armagan and Zaretzki (2011), the coordinate ascent variational inference algorithm for classical mean-field variational Bayes is equivalent to an EM algorithm for $p(\beta|y)$ with missing data z , which in this case is guaranteed to converge to the unique maximizer of $p(\beta|y)$ by, e.g., Theorem 3.2 of McLachlan and Krishnan (2007) and the fact that $p(\beta|y)$ is strictly concave (Haberman, 1974). Therefore $E_{q_{\text{mf}}^*(\beta)}(\beta) = \bar{\beta}^*$ and Lemma 5 implies that $\nu_p^{-1} \|E_{q_{\text{mf}}^*(\beta)}(\beta)\| \xrightarrow{a.s.} 0$ as $p \rightarrow \infty$.

We now show that $\nu_p^{-2} \|E_{p(\beta|y)}(\beta)\|^2 \xrightarrow{a.s.} [(\alpha \sigma_x^2)/(1 + \alpha \sigma_x^2)] c^2 n$ as $p \rightarrow \infty$. By the law of total expectation we have that $E_{p(\beta|y)}(\beta) = VX^\top E_{p(z|y)}(z)$, which implies

$$\|E_{p(\beta|y)}(\beta)\|^2 = E_{p(z|y)}(z)^\top XV^\top VX^\top E_{p(z|y)}(z).$$

Applying the Woodbury's identity to V we have $VX^\top = \nu_p^2 X^\top (I_n + \nu_p^2 XX^\top)^{-1}$. Hence, we can write $XV^\top VX^\top = (1 + \sigma_x^2 p \nu_p^2)^{-2} \sigma_x^2 p \nu_p^4 S^\top (\sigma_x^2 p)^{-1} XX^\top S$ with $S = (1 + \sigma_x^2 p \nu_p^2) (I_n + \nu_p^2 XX^\top)^{-1}$. Since $S^\top (\sigma_x^2 p)^{-1} XX^\top S \xrightarrow{a.s.} I_n$ as $p \rightarrow \infty$ by Lemma 2, it follows that

$$\lim_{p \rightarrow \infty} \nu_p^{-2} \|E_{p(\beta|y)}(\beta)\|^2 \stackrel{a.s.}{=} \lim_{p \rightarrow \infty} [(\sigma_x^2 p \nu_p^2)/(1 + \sigma_x^2 p \nu_p^2)] \|E_{p(z|y)}[(1 + \sigma_x^2 p \nu_p^2)^{-1/2} z]\|^2.$$

Since $(z | y) \sim \text{TN}[0, (I_n + \nu_p^2 XX^\top), \mathbb{A}]$, we have that $[(1 + \sigma_x^2 p \nu_p^2)^{-1/2} z | y] \sim \text{TN}[0, (1 + \sigma_x^2 p \nu_p^2)^{-1} (I_n + \nu_p^2 XX^\top), \mathbb{A}]$. Then,

$$E_{p(z_i|y)}[(1 + \sigma_x^2 p \nu_p^2)^{-1/2} z_i] = (1/\tilde{\psi}^{(p)}) \int_{\mathbb{A}} \tilde{u}_i \phi_n[\tilde{u}; (1 + \sigma_x^2 p \nu_p^2)^{-1} (I_n + \nu_p^2 XX^\top)] d\tilde{u},$$

where $\tilde{\psi}^{(p)} = \text{pr}(u^{(p)} \in \mathbb{A})$ for $u^{(p)} \sim \text{N}_n[0, (1 + \sigma_x^2 p \nu_p^2)^{-1} (I_n + \nu_p^2 XX^\top)]$. Thus, Lemma 2 together with a domination argument similar to the one used in the proof of Lemma 4 imply that, as $p \rightarrow \infty$,

$$E_{p(z_i|y)}[(1 + \sigma_x^2 p \nu_p^2)^{-1/2} z_i] \stackrel{a.s.}{\rightarrow} 2^n \int_{\mathbb{A}} \tilde{u}_i \phi_n(\tilde{u}; I_n) d\tilde{u} = c(2y_i - 1), \text{ with } c = 2 \int_0^\infty u \phi(u) du.$$

Thus, $\lim_{p \rightarrow \infty} \nu_p^{-2} \|E_{p(\beta|y)}(\beta)\|^2 \stackrel{a.s.}{=} [(\alpha\sigma_x^2)/(1 + \alpha\sigma_x^2)] \sum_{i=1}^n c^2 = [(\alpha\sigma_x^2)/(1 + \alpha\sigma_x^2)] c^2 n$.

Now, we prove $\liminf_{p \rightarrow \infty} \text{KL}[q_{\text{MF}}^*(\beta) \parallel p(\beta | y)] \stackrel{a.s.}{>} 0$. As a direct consequence of Lemma 6 we have that $\text{KL}[q_{\text{MF}}^*(\beta) \parallel p(\beta | y)] \geq 2 |\text{pr}_{\text{MF}} - \text{pr}_{\text{SUN}}|^2$, with $\text{pr}_{\text{SUN}} = \int \Phi(x_{\text{NEW}}^T \beta) p(\beta|y) d\beta$ and $\text{pr}_{\text{MF}} = \int \Phi(x_{\text{NEW}}^T \beta) q_{\text{MF}}^*(\beta) d\beta$. To continue the proof, we consider the input $x_{\text{NEW}} = (1 + \sigma_x^2 p \nu_p^2)^{-1/2} X^T H^{-1} \delta$, with $\delta = (2y_1 - 1, 0, \dots, 0)^T$, and show that $\lim_{p \rightarrow \infty} |\text{pr}_{\text{MF}} - \text{pr}_{\text{SUN}}| > 0$. Here we can assume without loss of generality that H is invertible because $H \stackrel{a.s.}{\rightarrow} [(\alpha\sigma_x^2)/(1 + \alpha\sigma_x^2)] I_n$ as $p \rightarrow \infty$ by Lemma 3 and the set of $n \times n$ non-singular matrices is open. This implies that H is eventually invertible as $p \rightarrow \infty$ almost surely. By definition of x_{NEW} we have

$$\nu_p^2 \|x_{\text{NEW}}\|^2 = \nu_p^2 x_{\text{NEW}}^T x_{\text{NEW}} = \frac{\sigma_x^2 p \nu_p^2}{1 + \sigma_x^2 p \nu_p^2} \delta^T H^{-1} (\sigma_x^2 p)^{-1} X X^T H^{-1} \delta \stackrel{a.s.}{\rightarrow} \frac{1 + \alpha\sigma_x^2}{\alpha\sigma_x^2} \quad \text{as } p \rightarrow \infty,$$

because $H^{-1} \stackrel{a.s.}{\rightarrow} [(1 + \alpha\sigma_x^2)/(\alpha\sigma_x^2)] I_n$ and $(\sigma_x^2 p)^{-1} X X^T \stackrel{a.s.}{\rightarrow} I_n$ as $p \rightarrow \infty$ by Lemmas 3 and 2, respectively, and $\|\delta\| = 1$. By (7) we have $\text{pr}_{\text{MF}} = \Phi[x_{\text{NEW}}^T \tilde{\beta}^* (1 + x_{\text{NEW}}^T V x_{\text{NEW}})^{-1/2}]$, and by Cauchy–Schwarz inequality and $x_{\text{NEW}}^T V x_{\text{NEW}} \geq 0$ we have $|x_{\text{NEW}}^T \tilde{\beta}^* (1 + x_{\text{NEW}}^T V x_{\text{NEW}})^{-1/2}| \leq \|x_{\text{NEW}}\| \|\tilde{\beta}^*\| \stackrel{a.s.}{\rightarrow} 0$ as $p \rightarrow \infty$, where the latter convergence follows from $\nu_p \|x_{\text{NEW}}\| \stackrel{a.s.}{\rightarrow} [(1 + \alpha\sigma_x^2)/\alpha\sigma_x^2]^{1/2} \in (1, \infty)$ and $\nu_p^{-1} \|\tilde{\beta}^*\| \stackrel{a.s.}{\rightarrow} 0$. Thus $\text{pr}_{\text{MF}} \stackrel{a.s.}{\rightarrow} 0.5$ as $p \rightarrow \infty$.

Consider now pr_{SUN} . With derivations analogous to those of equation (11), we can define pr_{SUN} as $\text{pr}_{\text{SUN}} = \mathbb{E}_{p(z|y)} \{\Phi[x_{\text{NEW}}^T V X^T z (1 + x_{\text{NEW}}^T V x_{\text{NEW}})^{-1/2}]\}$. By definition of x_{NEW} , we have that $x_{\text{NEW}}^T V x_{\text{NEW}} = (1 + \sigma_x^2 p \nu_p^2)^{-1} \delta^T H^{-1} \delta$ and, as $p \rightarrow \infty$, $H^{-1} \stackrel{a.s.}{\rightarrow} [(1 + \alpha\sigma_x^2)/(\alpha\sigma_x^2)] I_n$ by Lemma 3. Thus, $x_{\text{NEW}}^T V x_{\text{NEW}} \stackrel{a.s.}{\rightarrow} 0$ if $\alpha = \infty$, while $x_{\text{NEW}}^T V x_{\text{NEW}} \stackrel{a.s.}{\rightarrow} (\alpha\sigma_x^2)^{-1}$ if $\alpha \in (0, \infty)$. Moreover, $x_{\text{NEW}}^T V X^T z = \delta^T [(1 + \sigma_x^2 p \nu_p^2)^{-1/2} z]$ and $(1 + \sigma_x^2 p \nu_p^2)^{-1/2} z \rightarrow \text{TN}(0, I_n, \mathbb{A})$ in distribution as $p \rightarrow \infty$, almost surely. Combining these results with Slutsky’s lemma and the fact that $\Phi(\cdot)$ is bounded and continuous, it follows that $\mathbb{E}_{p(z|y)} \{\Phi[x_{\text{NEW}}^T V X^T z (1 + x_{\text{NEW}}^T V x_{\text{NEW}})^{-1/2}]\} \stackrel{a.s.}{\rightarrow} \mathbb{E}_{p(\tilde{z})} \{\Phi[\sqrt{\alpha\sigma_x^2(1 + \alpha\sigma_x^2)^{-1}} \tilde{z}]\}$ with $\tilde{z} \sim \text{TN}(0, I_n, \mathbb{A})$. Thus

$$\text{pr}_{\text{SUN}} \stackrel{a.s.}{\rightarrow} \mathbb{E}_{p(\tilde{z}_1)} \{\Phi[(2y_1 - 1) \sqrt{\alpha\sigma_x^2(1 + \alpha\sigma_x^2)^{-1}} \tilde{z}_1]\} = \int_0^\infty \Phi[\sqrt{\alpha\sigma_x^2(1 + \alpha\sigma_x^2)^{-1}} z] \cdot 2\phi(z) dz,$$

as $p \rightarrow \infty$, where $\Phi[\sqrt{\alpha\sigma_x^2(1 + \alpha\sigma_x^2)^{-1}} z] \cdot 2\phi(z) dz > 0.5$. Therefore, It directly follows that $\liminf_{p \rightarrow \infty} \text{KL}[q_{\text{MF}}^*(\beta) \parallel p(\beta | y)] \geq 2 \lim_{p \rightarrow \infty} |\text{pr}_{\text{MF}} - \text{pr}_{\text{SUN}}|^2 > 0$ almost surely as $p \rightarrow \infty$.

To conclude the proof of Theorem 1, note that, consistent with the above derivations, by setting $x_{\text{NEW}} = (1 + \sigma_x^2 p \nu_p^2)^{-1/2} X^T H^{-1} \delta$ with $\delta = (2y_1 - 1, 0, \dots, 0)^T$ for every p leads to $\liminf_{p \rightarrow \infty} |\text{pr}_{\text{MF}} - \text{pr}_{\text{SUN}}| > 0$, a.s., which proves the result on the predictive probabilities. \square

B.2 Proof of Theorem 2, Corollary 1 and Proposition 2

Proof of Theorem 2 Leveraging the chain rule of the KL divergence we have that

$$\text{KL}[q_{\text{PFM}}(\beta, z) \parallel p(\beta, z | y)] = \text{KL}[q_{\text{PFM}}(z) \parallel p(z | y)] + \mathbb{E}_{q_{\text{PFM}}(z)} \{\text{KL}[q_{\text{PFM}}(\beta | z) \parallel p(\beta | z)]\},$$

where $q_{\text{PFM}}(\beta|z)$ appears only in the second summand. This summand is always non-negative and coincides with zero, for every $q_{\text{PFM}}(z)$, if and only if $q_{\text{PFM}}^*(\beta | z) = p(\beta | z) = \phi_p(\beta - V X^T z; V)$.

The expression for $q_{\text{PFM}}^*(z) = \prod_{i=1}^n q_{\text{PFM}}^*(z_i)$ is instead a direct consequence of the closure under conditioning property of the multivariate truncated Gaussian (Horrace, 2005; Holmes and Held, 2006). In particular, adapting the results in Holmes and Held (2006), it easily follows that

$$p(z_i | z_{-i}, y) \propto \phi[z_i - (1 - x_i^T V x_i)^{-1} x_i^T V X_{-i}^T z_{-i}; (1 - x_i^T V x_i)^{-1}] 1[(2y_i - 1)z_i > 0],$$

for every $i = 1, \dots, n$, where X_{-i} is the design matrix without row i . To obtain the expression for $q_{\text{PFM}}^*(z_i)$, $i = 1, \dots, n$, note that, recalling e.g., Blei et al. (2017), the optimal solution for $q_{\text{PFM}}(z)$ which minimizes $\text{KL}[q_{\text{PFM}}(z) \parallel p(z | y)]$ within the family of distributions that factorize over z_1, \dots, z_n can be expressed as $\prod_{i=1}^n q_{\text{PFM}}^*(z_i)$ with $q_{\text{PFM}}^*(z_i) \propto \exp[\mathbb{E}_{q_{\text{PFM}}^*(z_{-i})}(\log[p(z_i | z_{-i}, y)])]$ for every $i = 1, \dots, n$. Combining such a result with the above expression for $p(z_i | z_{-i}, y)$ we have that $\exp[\mathbb{E}_{q_{\text{PFM}}^*(z_{-i})}(\log[p(z_i | z_{-i}, y)])]$ is proportional to

$$\exp\left[-\frac{z_i^2 - 2z_i(1 - x_i^T V x_i)^{-1} x_i^T V X_{-i}^T \mathbb{E}_{q_{\text{PFM}}^*(z_{-i})}(z_{-i})}{2(1 - x_i^T V x_i)^{-1}}\right] 1[(2y_i - 1)z_i > 0], \quad i = 1, \dots, n.$$

The above quantity coincides with the kernel of a Gaussian density having variance $\sigma_i^{*2} = (1 - x_i^T V x_i)^{-1}$, expectation $\mu_i^* = \sigma_i^{*2} x_i^T V X_{-i}^T \mathbb{E}_{q_{\text{PFM}}^*(z_{-i})}(z_{-i})$ and truncation below zero if $y_i = 1$ or above zero if $y_i = 0$. Hence, each $q_{\text{PFM}}^*(z_i)$ is the density of a truncated normal with parameters

specified as in Theorem 2. The proof is concluded after noticing that the expression for $\bar{z}_i^* = \mathbb{E}_{q_{\text{PFM}}^*(z_i)}(z_i)$, $i = 1, \dots, n$, in Theorem 2 follows directly from the mean of truncated normals. \square

Proof of Corollary 1 From (8), we have that $q_{\text{PFM}}^*(\beta)$ coincides with the density of a random variable that has the same distribution of $\tilde{u}^{(0)} + VX^T\tilde{u}^{(1)}$, where $\tilde{u}^{(0)} \sim N_p(0, V)$ and $\tilde{u}^{(1)}$ is from an n -variate Gaussian with mean vector μ^* , diagonal covariance matrix σ^{*2} and generic i th component truncated either below or above zero depending of the sign of $(2y_i - 1)$, for $i = 1, \dots, n$. Since $\tilde{u}^{(1)}$ has independent components, by standard properties of univariate truncated normal variables we obtain

$$\tilde{u}^{(0)} + VX^T\tilde{u}^{(1)} \stackrel{d}{=} u^{(0)} + VX^T\bar{Y}\sigma^*u^{(1)}, \quad \text{with } \bar{Y} = \text{diag}(2y_1 - 1, \dots, 2y_n - 1),$$

where $u^{(0)} \sim N_p(VX^T\mu^*, V)$ and $u^{(1)}$ is an n -variate Gaussian having mean vector 0, covariance matrix I_n , and truncation below $-\bar{Y}\sigma^{*-1}\mu^*$. Calling $\xi = VX^T\mu^*$, $\Omega = \omega\bar{\Omega}\omega = V + VX^T\sigma^{*2}XV$, $\Delta = \omega^{-1}VX^T\bar{Y}\sigma^*$, $\gamma = \bar{Y}\sigma^{*-1}\mu^*$ and $\Gamma = I_n$, as in Corollary 1, we have that

$$u^{(0)} + VX^T\bar{Y}\sigma^*u^{(1)} \stackrel{d}{=} \xi + \omega(\bar{u}^{(0)} + \Delta\Gamma^{-1}\bar{u}^{(1)}),$$

with $\bar{u}^{(0)} \sim N_p(\mathbf{0}, \bar{\Omega} - \Delta\Gamma^{-1}\Delta^T)$, and $\bar{u}^{(1)}$ distributed as a n -variate Gaussian random variable with mean vector $\mathbf{0}$, covariance matrix Γ , and truncation below $-\gamma$. Recalling [Arellano-Valle and Azzalini \(2006\)](#) and [Azzalini and Capitanio \(2014\)](#) such a stochastic representation coincides with the one of the unified skew-normal random variable $\text{SUN}_{p,n}(\xi, \Omega, \Delta, \gamma, \Gamma)$. \square

Proof of Proposition 2 To prove Proposition 2, first note that by the results in equation (8) and in Theorem 2, $z = (z_1, \dots, z_n)^T$ denotes a vector whose entries have independent truncated normal approximating densities. Hence, $\mathbb{E}_{q_{\text{PFM}}^*(z_i)}(z_i) = \bar{z}_i^*$ and $\text{var}_{q_{\text{PFM}}^*(z_i)}(z_i) = \sigma_i^{*2}[1 - (2y_i - 1)\eta_i^*\mu_i^*/\sigma_i^* - \eta_i^{*2}]$ with $\eta_i = \phi(\mu_i^*/\sigma_i^*)\Phi[(2y_i - 1)\mu_i^*/\sigma_i^*]^{-1}$ for $i = 1, \dots, n$. Using the parameters defined in Theorem 2, $\text{var}_{q_{\text{PFM}}^*(z_i)}(z_i)$ can be written as $\text{var}_{q_{\text{PFM}}^*(z_i)}(z_i) = \sigma_i^{*2} - (\bar{z}_i^* - \mu_i^*)\bar{z}_i^*$. Therefore, $\mathbb{E}_{q_{\text{PFM}}^*(z)}(z) = \bar{z}^*$ and $\text{var}_{q_{\text{PFM}}^*(z)}(z) = \text{diag}[\sigma_1^{*2} - (\bar{z}_1^* - \mu_1^*)\bar{z}_1^*, \dots, \sigma_n^{*2} - (\bar{z}_n^* - \mu_n^*)\bar{z}_n^*]$, where \bar{z}_i^* , μ_i^* and σ_i^* , $i = 1, \dots, n$ are defined in Theorem 2 and Corollary 1. Combining these results with equation (8), and using the law of iterated expectations we have

$$\begin{aligned} \mathbb{E}_{q_{\text{PFM}}^*(\beta)}(\beta) &= \mathbb{E}_{q_{\text{PFM}}^*(z)}[\mathbb{E}_{p(\beta|z)}(\beta)] = \mathbb{E}_{q_{\text{PFM}}^*(z)}(VX^Tz) = VX^T\mathbb{E}_{q_{\text{PFM}}^*(z)}(z) = VX^T\bar{z}^*, \\ \text{var}_{q_{\text{PFM}}^*(\beta)}(\beta) &= \mathbb{E}_{q_{\text{PFM}}^*(z)}[\text{var}_{p(\beta|z)}(\beta)] + \text{var}_{q_{\text{PFM}}^*(z)}[\mathbb{E}_{p(\beta|z)}(\beta)] = V + VX^T\text{var}_{q_{\text{PFM}}^*(z)}(z)XV \\ &= V + VX^T\text{diag}[\sigma_1^{*2} - (\bar{z}_1^* - \mu_1^*)\bar{z}_1^*, \dots, \sigma_n^{*2} - (\bar{z}_n^* - \mu_n^*)\bar{z}_n^*]XV, \end{aligned}$$

thus proving equation (10).

To prove equation (11) it suffices to notice that $\text{pr}_{\text{PFM}}(y_{\text{NEW}} = 1 | y) = \mathbb{E}_{q_{\text{PFM}}^*(\beta)}[\Phi(x_{\text{NEW}}^T\beta)]$. Hence, by applying again the law of iterated expectations we have

$$\begin{aligned} \mathbb{E}_{q_{\text{PFM}}^*(\beta)}[\Phi(x_{\text{NEW}}^T\beta)] &= \mathbb{E}_{q_{\text{PFM}}^*(z)}\{\mathbb{E}_{p(\beta|z)}[\Phi(x_{\text{NEW}}^T\beta)]\} \\ &= \mathbb{E}_{q_{\text{PFM}}^*(z)}\{\Phi[x_{\text{NEW}}^T VX^Tz(1 + x_{\text{NEW}}^T Vx_{\text{NEW}})^{-1/2}]\}. \end{aligned}$$

Last equality follows from the fact that $p(\beta | z)$ is a Gaussian density and thus $\mathbb{E}_{p(\beta|z)}[\Phi(x_{\text{NEW}}^T\beta)]$ can be derived in closed-form; see e.g., Lemma 7.1 in [Azzalini and Capitanio \(2014\)](#). \square

B.3 Proof of Theorem 3 and Corollary 2

Proof of Theorem 3 As a consequence of the discussion after the statement of Theorem 2, the density $q_{\text{PFM}}^*(z)$ minimizes the KL divergence to $p(z|y)$ within the family of distributions that factorize over z_1, \dots, z_n . Thus

$$\text{KL}[q_{\text{PFM}}^*(z) || p(z|y)] \leq \text{KL}[\text{TN}(0, (1 + \sigma_x^2 p\nu_p^2)I_n, \mathbb{A}) || p(z|y)] \quad (15)$$

Since the KL divergence is invariant with respect to bijective transformations and $p(z|y) = \text{TN}(0, I_n + \nu_p^2 XX^T, \mathbb{A})$, then rescaling each z_i by $(1 + \sigma_x^2 p\nu_p^2)^{-1/2}$ we have

$$\begin{aligned} &\text{KL}[\text{TN}(0, (1 + \sigma_x^2 p\nu_p^2)I_n, \mathbb{A}) || p(z|y)] \\ &= \text{KL}[\text{TN}(0, I_n, \mathbb{A}) || \text{TN}(0, (1 + \sigma_x^2 p\nu_p^2)^{-1}(I_n + \nu_p^2 XX^T), \mathbb{A})]. \end{aligned} \quad (16)$$

Lemma 2 shows that, under Assumptions 2–3, $(1 + \sigma_x^2 p \nu_p^2)^{-1} (I_n + \nu_p^2 X X^T) \xrightarrow{p} I_n$ and thus the continuous mapping theorem, combined with Lemma 4, implies that

$$\text{KL}[\text{TN}(0, I_n, \mathbb{A}) \parallel \text{TN}(0, (1 + \sigma_x^2 p \nu_p^2)^{-1} (I_n + \nu_p^2 X X^T), \mathbb{A})] \xrightarrow{p} 0 \quad (17)$$

as $p \rightarrow \infty$. Combining (15), (16) and (17) we obtain $\text{KL}[q_{\text{PFM}}^*(z) \parallel p(z|y)] \xrightarrow{p} 0$ as $p \rightarrow \infty$, as desired. \square

Proof of Corollary 2 Lemma 6 and Theorem 3 imply that, under Assumptions 2–3, we have

$$\text{pr} \left[\sup_{x_{\text{NEW}} \in \mathfrak{R}^p} |\text{pr}_{\text{PFM}} - \text{pr}_{\text{SUN}}| > \epsilon \right] \leq \text{pr} \{ \text{KL}[q_{\text{PFM}}^*(\beta) \parallel p(\beta | y)] > 2\epsilon^2 \} \rightarrow 0, \quad \text{as } p \rightarrow \infty$$

for any $\epsilon > 0$. \square

B.4 Proof of Theorem 4

Lemma 7 Let $y \in \{0; 1\}$ and $\bar{z}^* = \mu^* + (2y - 1)\sigma^* \phi(\mu^*/\sigma^*) \Phi[(2y - 1)\mu^*/\sigma^*]^{-1}$ be a function of $\mu^* \in \mathfrak{R}$ and $\sigma^* \geq 0$. Then $\sup_{\mu^*, \sigma^*} (|\mu^*| + \sigma^*)^{-1} |\bar{z}^*| < \infty$.

Proof. By the triangle inequality

$$(|\mu^*| + \sigma^*)^{-1} |\bar{z}^*| \leq 1 + (|\mu^*| + \sigma^*)^{-1} \sigma^* \phi(|\mu^*|/\sigma^*) / \Phi(-|\mu^*|/\sigma^*).$$

If $|\mu^*| \leq \sigma^*$ then $|\bar{z}^*|/(|\mu^*| + \sigma^*) \leq 1 + 1 \times \phi(0) / \Phi(-1) < \infty$. If $|\mu^*| > \sigma^*$, setting $t = |\mu^*|/\sigma^*$ and using the bound $\Phi(-t) \geq (2\pi)^{-1/2} t(t^2 + 1)^{-1} \exp(-t^2/2)$, which holds for every $t > 0$, we have

$$\begin{aligned} (|\mu^*| + \sigma^*)^{-1} |\bar{z}^*| &\leq 1 + |\mu^*|^{-1} \sigma^* \phi(t) / \Phi(-t) \\ &\leq 1 + t^{-1} \exp(-t^2/2) [(t^2 + 1)^{-1} t \exp(-t^2/2)]^{-1} = 1 + t^{-2} (t^2 + 1) < 3 \end{aligned}$$

where in the last inequality we have used $t > 1$. Combining the above results it follows that $\sup_{\mu^*, \sigma^*} (|\mu^*| + \sigma^*)^{-1} |\bar{z}^*| < \infty$ as desired. \square

Lemma 8 Under Assumptions 2 and 3, for every statistical unit $i = 1, \dots, n$, we have $(1 + \sigma_x^2 p \nu_p^2)^{-1/2} \mu_i^{(1)} \xrightarrow{p} 0$ as $p \rightarrow \infty$, where $\mu_i^{(1)}$ is defined as in Algorithm 2.

Proof. Case a) $\alpha = \infty$. For any $i = 1, \dots, n$, we have

$$\frac{|\bar{z}_i^{(0)}|}{(1 + \sigma_x^2 p \nu_p^2)^{1/2}} = \frac{|\bar{z}_i^{(0)}|}{|\mu_i^{(0)}| + \sigma_i^*} \frac{|\mu_i^{(0)}| + \sigma_i^*}{(1 + \sigma_x^2 p \nu_p^2)^{1/2}} \leq C \frac{|\mu_i^{(0)}| + \sigma_i^*}{(1 + \sigma_x^2 p \nu_p^2)^{1/2}}, \quad (18)$$

where $C = \sup_{\mu^*, \sigma^*} (|\mu^*| + \sigma^*)^{-1} |\bar{z}^*| < \infty$ by Lemma 7. Moreover

$$\frac{|\mu_i^{(0)}| + \sigma_i^*}{(1 + \sigma_x^2 p \nu_p^2)^{1/2}} \xrightarrow{p} 1 \quad \text{as } p \rightarrow \infty, \quad (19)$$

because $(1 + \sigma_x^2 p \nu_p^2)^{-1/2} \sigma_i^* \xrightarrow{p} 1$ as $p \rightarrow \infty$ by $\sigma_i^* = (1 - H_{ii})^{-1/2}$ and Lemma 3, while $(1 + \sigma_x^2 p \nu_p^2)^{-1/2} \mu_i^{(0)} \rightarrow 0$ as $p \rightarrow \infty$ since $\alpha = \infty$. Note that we are implicitly assuming Algorithm 2 to have fixed initialization $(\mu_1^{(0)}, \dots, \mu_n^{(0)}) \in \mathfrak{R}^n$, obtained from $(\bar{z}_1^{(0)}, \dots, \bar{z}_n^{(0)}) \in \mathfrak{R}^n$. It follows by (18) and (19) that

$$\text{pr}[(1 + \sigma_x^2 p \nu_p^2)^{-1/2} |\bar{z}_i^{(0)}| > C + \epsilon] \rightarrow 0 \quad \text{as } p \rightarrow \infty \text{ for any } \epsilon > 0. \quad (20)$$

We now prove that $(1 + \sigma_x^2 p \nu_p^2)^{-1/2} \mu_i^{(1)} \xrightarrow{p} 0$ and $\text{pr}[(1 + \sigma_x^2 p \nu_p^2)^{-1/2} |\bar{z}_i^{(1)}| > C + \epsilon] \rightarrow 0$ as $p \rightarrow \infty$, for any $\epsilon > 0$ and for every $i = 1, \dots, n$. We proceed by induction on i . Recalling the definition of $\mu_1^{(1)}$ in Algorithm 2, we have that

$$(1 + \sigma_x^2 p \nu_p^2)^{-1/2} \mu_1^{(1)} = \sum_{i'=2}^n \sigma_1^{*2} H_{1i'} (1 + \sigma_x^2 p \nu_p^2)^{-1/2} \bar{z}_{i'}^{(0)} \quad (21)$$

Also,

$$\sigma_i^{*2} H_{ii'} = [(1 + \sigma_x^2 p \nu_p^2)(1 - H_{ii})]^{-1} \cdot [(1 + \sigma_x^2 p \nu_p^2) H_{ii'}] \xrightarrow{p} 0 \quad (22)$$

as $p \rightarrow \infty$ for every $i \neq i'$ since, by Lemma 3, the first and second factors converge in probability to 1 and 0, respectively. By (20) and (22) we have $\sigma_1^{*2} H_{1i'} (1 + \sigma_x^2 p \nu_p^2)^{-1/2} \bar{z}_{i'}^{(0)} \xrightarrow{p} 0$ as $p \rightarrow \infty$ for every $i' \geq 2$. Thus, by (21), also $(1 + \sigma_x^2 p \nu_p^2)^{-1/2} \mu_1^{(1)} \xrightarrow{p} 0$ as $p \rightarrow \infty$. Finally, the statement $\text{pr}\{(1 + \sigma_x^2 p \nu_p^2)^{-1/2} |\bar{z}_1^{(1)}| > C + \epsilon\} \rightarrow 0$ as $p \rightarrow \infty$ for any $\epsilon > 0$ follows from $|(1 + \sigma_x^2 p \nu_p^2)^{-1/2} \mu_1^{(1)}| \xrightarrow{p} 0$ as $p \rightarrow \infty$ and arguments analogous to the ones in (18) and (19). We thus proved the desired induction statement for $i = 1$. When $i \geq 2$ we have

$$\begin{aligned} & (1 + \sigma_x^2 p \nu_p^2)^{-1/2} \mu_i^{(1)} \\ &= \sum_{i'=1}^{i-1} \sigma_i^{*2} H_{ii'} (1 + \sigma_x^2 p \nu_p^2)^{-1/2} \bar{z}_{i'}^{(1)} + \sum_{i'=i+1}^n \sigma_i^{*2} H_{ii'} (1 + \sigma_x^2 p \nu_p^2)^{-1/2} \bar{z}_{i'}^{(0)}. \end{aligned} \quad (23)$$

For $i' > i$ we have

$$\sigma_i^{*2} H_{ii'} (1 + \sigma_x^2 p \nu_p^2)^{-1/2} \bar{z}_{i'}^{(0)} \xrightarrow{p} 0, \quad \text{as } p \rightarrow \infty,$$

by (20) and (22). Instead, for $i' < i$ we have

$$\sigma_i^{*2} H_{ii'} (1 + \sigma_x^2 p \nu_p^2)^{-1/2} \bar{z}_{i'}^{(1)} \xrightarrow{p} 0, \quad \text{as } p \rightarrow \infty,$$

since $\sigma_i^{*2} H_{ii'} \xrightarrow{p} 0$ as $p \rightarrow \infty$ by (20) and $\text{pr}\{(1 + \sigma_x^2 p \nu_p^2)^{-1/2} |\bar{z}_{i'}^{(1)}| > C + \epsilon\} \rightarrow 0$ as $p \rightarrow \infty$ for every $\epsilon > 0$ by the inductive hypothesis. Combining these results, it follows by (23) that $(1 + \sigma_x^2 p \nu_p^2)^{-1/2} \mu_i^{(1)} \xrightarrow{p} 0$ and thus that $\text{pr}\{(1 + \sigma_x^2 p \nu_p^2)^{-1/2} |\bar{z}_i^{(1)}| > C + \epsilon\} \rightarrow 0$ as $p \rightarrow \infty$ by arguments analogous to the ones in (18) and (19). The thesis follows by induction.

Case b) $\alpha \in (0, \infty)$. Here, the stronger result $\mu_i^{(1)} \xrightarrow{p} 0$ as $p \rightarrow \infty$ holds. The proof follows the same steps of the previous case. First, adapting the derivations above, for every $i = 1, \dots, n$, we have

$$|\bar{z}_i^{(0)}| = \frac{|\bar{z}_i^{(0)}|}{|\mu_i^{(0)}| + \sigma_i^*} (|\mu_i^{(0)}| + \sigma_i^*) \leq C (|\mu_i^{(0)}| + \sigma_i^*), \quad (24)$$

where $C = \sup_{\mu^*, \sigma^*} (|\mu^*| + \sigma^*)^{-1} |\bar{z}^*| < \infty$ by Lemma 7. Moreover,

$$\sigma_i^* \xrightarrow{p} (1 + \alpha \sigma_x^2)^{1/2}, \quad (25)$$

by $\sigma_i^* = (1 - H_{ii})^{-1/2}$ and Lemma 3. Thus, calling $M = \max_{i=1, \dots, n} |\mu_i^{(0)}| < \infty$, it follows by (24) and (25) that

$$\text{pr}\{|\bar{z}_i^{(0)}| > C[M + (1 + \alpha \sigma_x^2)^{1/2} + \epsilon]\} \rightarrow 0 \quad \text{as } p \rightarrow \infty \text{ for any } \epsilon > 0. \quad (26)$$

Adapting the proof of the previous case, we now prove that $\mu_i^{(1)} \xrightarrow{p} 0$ and $\text{pr}\{|\bar{z}_i^{(1)}| > C[(1 + \alpha \sigma_x^2)^{1/2} + \epsilon]\} \rightarrow 0$ as $p \rightarrow \infty$, for any $\epsilon > 0$ and for every $i = 1, \dots, n$. We proceed by induction on i . Recalling the definition of $\mu_1^{(1)}$ in Algorithm 2, we have that

$$\mu_1^{(1)} = \sum_{i'=2}^n \sigma_1^{*2} H_{1i'} \bar{z}_{i'}^{(0)}. \quad (27)$$

Since the arguments leading to Equation (22) hold also in this case, by (22) and (26) we have $\sigma_1^{*2} H_{1i'} \bar{z}_{i'}^{(0)} \xrightarrow{p} 0$ as $p \rightarrow \infty$ for every $i' \geq 2$. Thus, by (27), also $\mu_1^{(1)} \xrightarrow{p} 0$ as $p \rightarrow \infty$. Finally, the statement $\text{pr}\{|\bar{z}_1^{(1)}| > C[(1 + \alpha \sigma_x^2)^{1/2} + \epsilon]\} \rightarrow 0$ as $p \rightarrow \infty$ for any $\epsilon > 0$ follows from $|\mu_1^{(1)}| \xrightarrow{p} 0$ as $p \rightarrow \infty$ and arguments analogous to the ones in (24) and (25). The desired induction statement for $i = 1$ has thus been proved. When $i \geq 1$ we have

$$\mu_i^{(1)} = \sum_{i'=1}^{i-1} \sigma_i^{*2} H_{ii'} \bar{z}_{i'}^{(1)} + \sum_{i'=i+1}^n \sigma_i^{*2} H_{ii'} \bar{z}_{i'}^{(0)}. \quad (28)$$

For $i' > i$ we have that $\sigma_i^{*2} H_{ii'} \bar{z}_{i'}^{(0)} \xrightarrow{p} 0$ as $p \rightarrow \infty$ by (26) and (22). For $i' < i$ we have $\sigma_i^{*2} H_{ii'} \bar{z}_{i'}^{(1)} \xrightarrow{p} 0$ as $p \rightarrow \infty$ since $\sigma_i^{*2} H_{ii'} \xrightarrow{p} 0$ as $p \rightarrow \infty$ by (20) and $\text{pr}\{|\bar{z}_{i'}^{(1)}| > C[(1 + \alpha \sigma_x^2)^{1/2} + \epsilon]\} \rightarrow 0$ as $p \rightarrow \infty$ for every $\epsilon > 0$ by the inductive hypothesis. It follows by (28) that $\mu_i^{(1)} \xrightarrow{p} 0$ and thus that $\text{pr}\{|\bar{z}_i^{(1)}| > C[(1 + \alpha \sigma_x^2)^{1/2} + \epsilon]\} \rightarrow 0$ as $p \rightarrow \infty$ by arguments analogous to the ones in (24) and (25). The thesis follows by induction. \square

Proof of Theorem 4 By leveraging the chain rule for KL divergences and the fact that $q_{\text{PFM}}^{(1)}(\beta|z) = p(\beta|y, z)$ we have

$$\begin{aligned} \text{KL}[q_{\text{PFM}}^{(1)}(\beta) \parallel p(\beta|y)] &\leq \text{KL}[q_{\text{PFM}}^{(1)}(\beta) \parallel p(\beta|y)] + \mathbb{E}_{q_{\text{PFM}}^{(1)}(\beta)} \{ \text{KL}[q_{\text{PFM}}^{(1)}(z | \beta) \parallel p(z | y, \beta)] \} \\ &= \text{KL}[q_{\text{PFM}}^{(1)}(z) \parallel p(z | y)] + \mathbb{E}_{q_{\text{PFM}}^{(1)}(z)} \{ \text{KL}[q_{\text{PFM}}^{(1)}(\beta | z) \parallel p(\beta | y, z)] \} \\ &= \text{KL}[q_{\text{PFM}}^{(1)}(z) \parallel p(z|y)]. \end{aligned}$$

Since $q_{\text{PFM}}^{(1)}(z) = \text{TN}(\mu^{(1)}, \sigma^{*2}, \mathbb{A})$, $p(z|y) = \text{TN}[0, (I_n + \nu_p^2 X X^T), \mathbb{A}]$ and the KL divergence is invariant with respect to bijective transformations, then, calling $k_p = (1 + \sigma_x^2 p \nu_p)$ and rescaling each z_i by $k_p^{-1/2}$ we get

$$\text{KL}[q_{\text{PFM}}^{(1)}(z) \parallel p(z|y)] = \text{KL}[\text{TN}(k_p^{-1/2} \mu^{(1)}, k_p^{-1} \sigma^{*2}, \mathbb{A}) \parallel \text{TN}[0, k_p^{-1} (I_n + \nu_p^2 X X^T), \mathbb{A}]].$$

Lemma 8 implies that $k_p^{-1/2} \mu^{(1)} \xrightarrow{p} 0$ as $p \rightarrow \infty$, while Lemmas 2 and 3 imply that both $k_p^{-1} (I_n + \nu_p^2 X X^T)$ and $k_p^{-1} \sigma^{*2}$ converge in probability to I_n as $p \rightarrow \infty$. Therefore

$$\text{KL}[\text{TN}(k_p^{-1/2} \mu^{(1)}, k_p^{-1} \sigma^{*2}, \mathbb{A}) \parallel \text{TN}[0, k_p^{-1} (I_n + \nu_p^2 X X^T), \mathbb{A}]] \xrightarrow{p} 0$$

by Lemma 4 and the continuous mapping theorem, implying $\text{KL}[q_{\text{PFM}}^{(1)}(\beta) \parallel p(\beta|y)] \xrightarrow{p} 0$ as $p \rightarrow \infty$, as desired. \square

C Additional Simulation Studies

We consider here additional simulation studies to check whether the findings reported in the article apply also to more general data structures which do not meet the assumptions we require to prove the theory in Sections 2.1–2.2 in the article. With this goal in mind, we replicate the simulation experiment in the article under two alternative generative mechanisms for the predictors in the design matrix X , which avoid assuming independence across columns and rows. More specifically, in the first alternative scenario we induce dependence across columns by simulating the n rows of X , excluding the intercept, from a $(p - 1)$ -variate Gaussian distribution with zero means, unit variances and pairwise correlations $\text{corr}(x_{ij}, x_{ij'}) = 0.5$, for each $j = 2, \dots, p$ and $j' = 2, \dots, p$. In the second alternative scenario, we induce instead correlation across statistical units by simulating the $p - 1$ columns of X , excluding the intercept, from an n -variate Gaussian with zero means, unit variances and decaying pairwise correlations $\text{corr}(x_{ij}, x_{i'j}) = 0.5^{(i-i')}$, for each $i = 1, \dots, n$ and $i' = 1, \dots, n$. These two scenarios feature strong correlations, arguably more extreme relative to the ones found in real-world applications. Hence, such an assessment provides an important stress test to evaluate the performance of the proposed partially-factorized variational Bayes and the classical mean-field variational Bayes in challenging regimes. For instance, the more structured dependence that we induce among units is meant to provide a highly challenging scenario in which standardization has almost no effect in reducing the correlation across rows. In fact, as discussed more in detail in Section 4 in the article, we found that the recommendations provided by Gelman et al. (2008) and Chopin and Ridgway (2017) on standardization are beneficial in reducing the correlation between the rows of X in routine real-world applications, thereby further improving the quality of the partially-factorized approximation. When standardization is implemented, we recommend to always include the intercept term which is crucial to account for the centering effects (e.g., Gelman et al., 2008; Chopin and Ridgway, 2017).

Figure S1 illustrates performance under these challenging regimes by reproducing an assessment analogous to Figure 1 in the article. According to Figure S1, the results are overall coherent with the evidence provided by Figure 1, for both approximations, meaning that the proposed partially-factorized strategy provides a powerful solution under a variety of challenging settings and the theoretical results in Sections 2.1–2.2 of the article match empirical evidence even beyond the assumptions we require for their proof. As one might expect, the partially-factorized approximation is slightly less accurate when there is correlation across the n units relative to scenarios with no correlation or correlation across the p predictors. Nonetheless, the approximation error relative to STAN Monte Carlo estimates is still very low also in such settings.

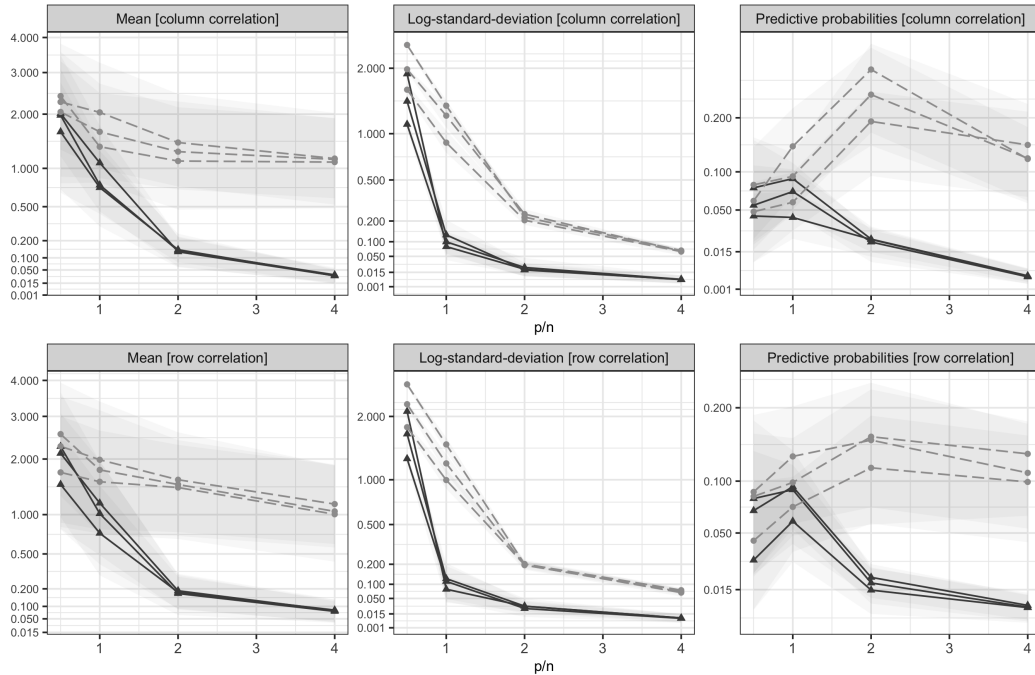


Figure S1: Accuracy in the approximation for three key functionals of the posterior distribution for β . Trajectories for the median of the absolute differences between an accurate but expensive Monte Carlo estimate of such functionals and their approximations provided by partially-factorized variational Bayes (dark grey solid lines) and mean-field variational Bayes (light grey dashed lines), respectively, for increasing values of the ratio p/n , i.e., $p/n \in \{0.5; 1; 2; 4\}$. The different trajectories for each of the two methods correspond to three different settings of the sample size n , i.e., $n \in \{50; 100; 250\}$, whereas the grey areas denote the first and third quartiles computed from the absolute differences. The two row panels correspond to simulation scenarios in which there is dependence across the different predictors defining the columns of X (first row), and dependence between the statistical units denoting the rows of X (second row). For graphical purposes we consider a square-root scale for the y -axis.

D Additional Medical Applications

We consider here additional analyses of the Alzheimer’s dataset in Section 4 in the article. Figure S2 complements the results in Figures 2 and 3 in the article, by comparing graphically the quality of the marginal approximation for the coefficients associated with the highest and lowest Wasserstein distance from the exact posterior under the two variational approximations analyzed. As is clear from Figure S2, partially-factorized variational Bayes produces approximations which perfectly overlap with the exact posterior in all cases, including also the worst-case scenario with the highest Wasserstein distance. Consistent with Theorem 1, the mean-field approximations has instead a reduced quality mostly due to a tendency to over-shrink towards zero the locations of the actual posterior.

To illustrate the performance of the two variational approximations for more structured priors controlling the variance of the entire linear predictor in the Alzheimer’s dataset, we also study the same quantities shown in Figure 3 in the article, when $\nu_p^2 = 25$ is replaced with $\nu_p^2 = 25 \cdot 100/p$ and $\nu_p^2 = 25 \cdot 10/p$, respectively. These choices control, heuristically, the total variance of the linear predictor as if there were respectively 100 and 10 coefficients, out of 9036, with prior standard deviation 5, while the others were fixed to zero. As illustrated in the first and last columns of Figure S3, when ν_p^2 decreases with p , also the exact posterior expectations increasingly shrink towards 0. Hence, the resulting bias in the mean-field approximation, that was dramatic in the constant-variance scenario, is less severe, though still evident even for $\nu_p^2 = 25 \cdot 10/p \approx 0.028$. On the other hand, the approximate functionals obtained under the partially-factorized solution still overlap perfectly with the exact quantities in all scenarios. The quality in the approximation of the standard deviations is instead comparable to the results discussed in Figure 3.

We conclude our studies by providing further evidence for the behavior of the two variational approximations in settings where the main focus is accurate prediction. With this goal in mind, we consider three additional medical datasets with different combinations of (n, p) available at the UCI Machine Learning Repository (<https://archive.ics.uci.edu/ml/datasets.php>). The first two studies focus on Parkinson’s disease and its relation with speech recordings to detect dis-

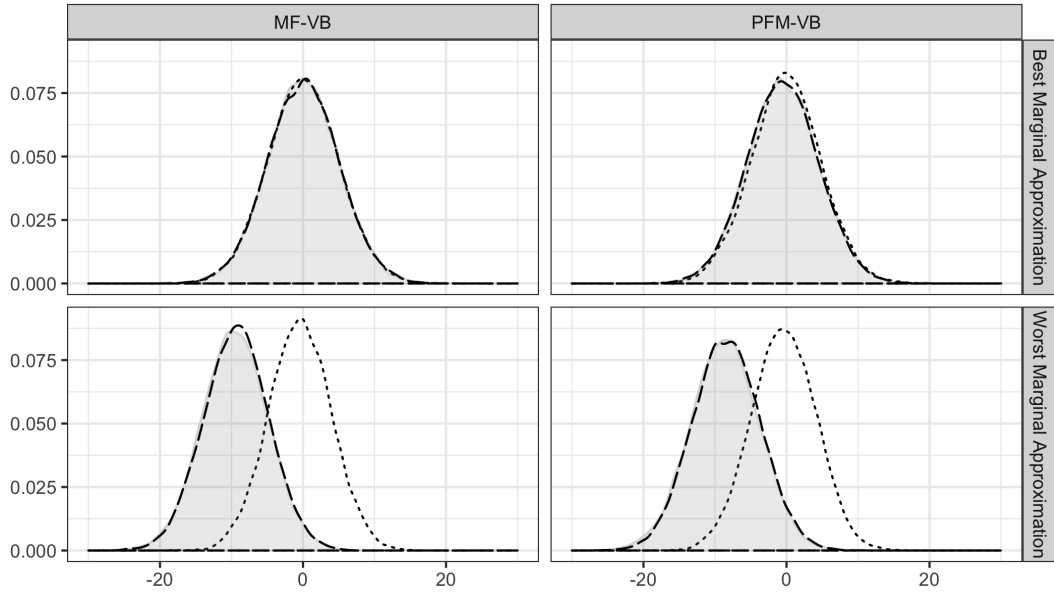


Figure S2: Quality of the marginal approximation for the coefficients associated with the highest and lowest Wasserstein distance from the exact posterior under mean-field variational Bayes (MF-VB) and partially-factorized variational Bayes (PFM-VB), respectively. The shaded grey area denotes the density of the exact posterior marginal, whereas the dotted and dashed lines represent the approximate densities provided by mean-field and partially-factorized variational Bayes, respectively.

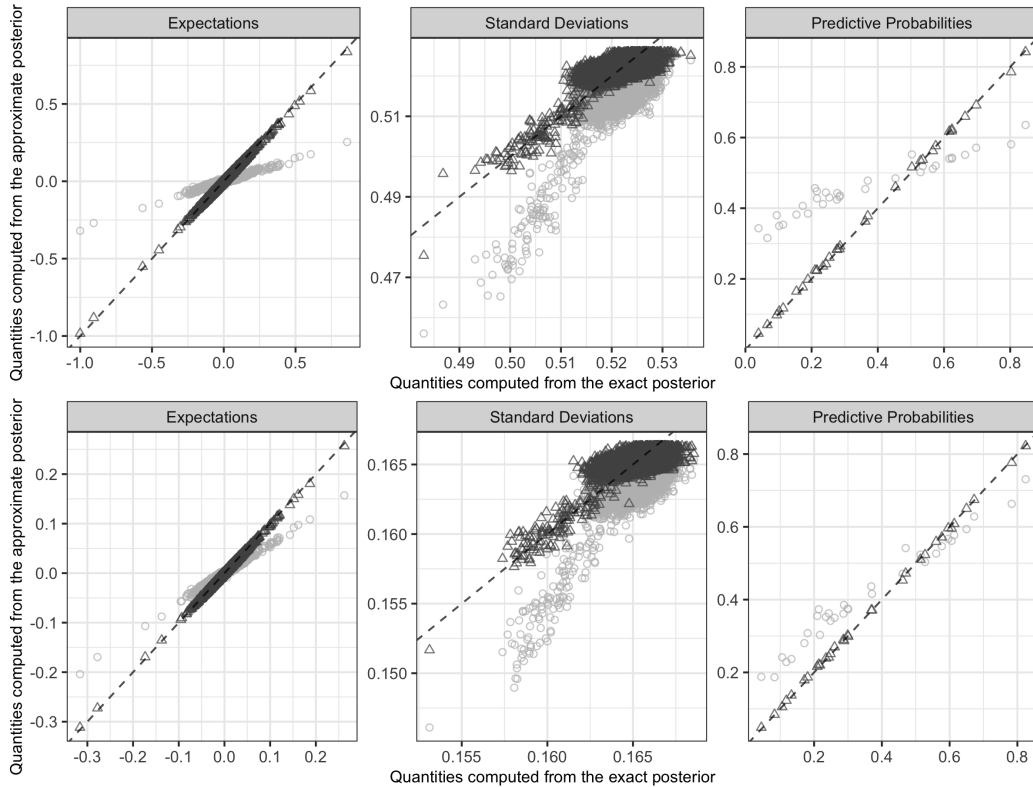


Figure S3: Scatterplots comparing the posterior expectations, standard deviations and predictive probabilities computed from 20000 values sampled from the exact SUN posterior, with those provided by mean-field variational Bayes (light grey circles) and partially-factorized variational Bayes (dark grey triangles). Upper panels represent the scenario $\nu_p^2 = 25 \cdot 100/p$, whereas the bottom ones consider the setting $\nu_p^2 = 25 \cdot 10/p$.

ease presence (parkinson, Sakar et al. (2019)) or to assess effectiveness of voice rehabilitation treatments (voice, Tsanas et al. (2013)). The third dataset refers instead to a study aimed at predicting whether a gastrointestinal lesion is benign or malignant as a function of textural, color and shape data (lesion, Mesejo et al. (2016)). To each of these datasets we apply model (1) with the

	parkinson ($n = 756, p = 754$)	voice ($n = 126, p = 310$)	lesion ($n = 76, p = 952$)
MF-VB	321.39	61.05	48.55
PFM-VB	305.28	46.49	27.14

Table S1: Five-fold cross-validation estimate of the test deviance for three different medical datasets, when the out-of-sample predictive probabilities are estimated under mean-field variational Bayes (MF-VB) and partially-factorized variational Bayes (PFM-VB), respectively.

same settings initially considered for the Alzheimer’s study, and evaluate predictive performance of classical mean-field approximation and the proposed partially-factorized alternative. Following common practice in machine learning, we consider five-fold cross-validation estimates of test deviances $-\sum_{i=1}^n \{y_i \log \hat{p}_{\text{MF}}(y_i = 1 | y_{\text{FOLD}(-i)}) + (1 - y_i) \log[1 - \hat{p}_{\text{MF}}(y_i = 1 | y_{\text{FOLD}(-i)})]\}$ and $-\sum_{i=1}^n \{y_i \log \hat{p}_{\text{PFM}}(y_i = 1 | y_{\text{FOLD}(-i)}) + (1 - y_i) \log[1 - \hat{p}_{\text{PFM}}(y_i = 1 | y_{\text{FOLD}(-i)})]\}$, for the mean-field and partially-factorized variational approximations, respectively, where $y_{\text{FOLD}(-i)}$ denotes the response vector for all the individuals which are not in the same fold of unit i . Such measures are reported in Table S1, and further confirm the substantially improved quality of the partially-factorized solution relative to the mean-field one, also when the focus is specifically on predictive inference. Consistent with the results in simulations and in the Alzheimer’s application in the article, such gains are found in all the three medical studies and become substantial as p grows relative to n . For instance, in the `voice` and `lesion` applications, the partially-factorized approximation reduces the test deviance of classical mean-field by 25% and 50%, respectively. In predictive inference, such a reduction is a notable improvement.

References

- Albert, J. H. and Chib, S. (1993). Bayesian analysis of binary and polychotomous response data. *Journal of the American Statistical Association*, 88:669–679.
- Arellano-Valle, R. B. and Azzalini, A. (2006). On the unification of families of skew-normal distributions. *Scandinavian Journal of Statistics*, 33:561–574.
- Armagan, A. and Zaretski, R. L. (2011). A note on mean-field variational approximations in Bayesian probit models. *Computational Statistics & Data Analysis*, 55(1):641–643.
- Azzalini, A. and Capitanio, A. (2014). *The Skew-normal and Related Families*. Cambridge University Press.
- Blei, D. M., Kucukelbir, A., and McAuliffe, J. D. (2017). Variational inference: A review for statisticians. *Journal of the American Statistical Association*, 112(518):859–877.
- Botev, Z. (2017). The normal law under linear restrictions: simulation and estimation via minimax tilting. *Journal of the Royal Statistical Society: Series B (Statistical Methodology)*, 79(1):125–148.
- Cao, J., Durante, D., and Genton, M. G. (2020). Scalable computation of predictive probabilities in probit models with Gaussian process priors. *arXiv preprint arXiv:2009.01471*.
- Cao, J., Genton, M. G., Keyes, D. E., and Turkiyyah, G. M. (2019). Hierarchical-block conditioning approximations for high-dimensional multivariate normal probabilities. *Statistics and Computing*, 29:585–598.
- Chipman, H. A., George, E. I., and McCulloch, R. E. (2010). BART: Bayesian additive regression trees. *The Annals of Applied Statistics*, 4:266–298.
- Chopin, N. (2011). Fast simulation of truncated Gaussian distributions. *Statistics and Computing*, 21(2):275–288.
- Chopin, N. and Ridgway, J. (2017). Leave Pima Indians alone: binary regression as a benchmark for Bayesian computation. *Statistical Science*, 32(1):64–87.
- Consonni, G. and Marin, J.-M. (2007). Mean-field variational approximate Bayesian inference for latent variable models. *Computational Statistics & Data Analysis*, 52:790–798.
- Craig-Schapiro, R., Kuhn, M., Xiong, C., Pickering, E. H., Liu, J., Misko, T. P., Perrin, R. J., Bales, K. R., Soares, H., and Fagan, A. M. (2011). Multiplexed immunoassay panel identifies novel CSF biomarkers for Alzheimer’s disease diagnosis and prognosis. *PLoS one*, 6(4):e18850.
- Durante, D. (2019). Conjugate Bayes for probit regression via unified skew-normal distributions. *Biometrika*, 106(4):765–779.
- Durante, D. and Rigon, T. (2019). Conditionally conjugate mean-field variational Bayes for logistic models. *Statistical Science*, 34(3):472–485.
- Fasano, A. and Durante, D. (2020). A class of conjugate priors for multinomial probit models which includes the multivariate normal one. *arXiv preprint arXiv:2007.06944*.

- Frühwirth-Schnatter, S. and Frühwirth, R. (2007). Auxiliary mixture sampling with applications to logistic models. *Computational Statistics & Data Analysis*, 51:3509–3528.
- Fuglstad, G.-A., Hem, I. G., Knight, A., Rue, H., and Riebler, A. (2018). Intuitive joint priors for variance parameters. *Bayesian Analysis*.
- Gelman, A., Jakulin, A., Pittau, M. G., and Su, Y.-S. (2008). A weakly informative default prior distribution for logistic and other regression models. *The Annals of Applied Statistics*, 2(4):1360–1383.
- Girolami, M. and Rogers, S. (2006). Variational Bayesian multinomial probit regression with Gaussian process priors. *Neural Computation*, 18:1790–1817.
- Haario, H., Saksman, E., and Tamminen, J. (2001). An adaptive Metropolis algorithm. *Bernoulli*, 7(2):223–242.
- Haberman, S. J. (1974). *The Analysis of Frequency Data*. University of Chicago Press, Chicago.
- Hoffman, M. D. and Gelman, A. (2014). The No-U-turn sampler: Adaptively setting path lengths in Hamiltonian Monte Carlo. *Journal of Machine Learning Research*, 15:1593–1623.
- Holmes, C. C. and Held, L. (2006). Bayesian auxiliary variable models for binary and multinomial regression. *Bayesian Analysis*, 1:145–168.
- Horrace, W. C. (2005). Some results on the multivariate truncated normal distribution. *Journal of Multivariate Analysis*, 94(1):209–221.
- Jaakkola, T. S. and Jordan, M. I. (2000). Bayesian parameter estimation via variational methods. *Statistics and Computing*, 10(1):25–37.
- Johndrow, J. E., Smith, A., Pillai, N., and Dunson, D. B. (2019). MCMC for imbalanced categorical data. *Journal of the American Statistical Association*, 114:1394–1403.
- Knowles, D. A. and Minka, T. (2011). Non-conjugate variational message passing for multinomial and binary regression. In *Advances in Neural Information Processing Systems*, pages 1701–1709.
- Kullback, S. and Leibler, R. A. (1951). On information and sufficiency. *The Annals of Mathematical Statistics*, 22:79–86.
- Kuss, M. and Rasmussen, C. E. (2005). Assessing approximate inference for binary Gaussian process classification. *Journal of Machine Learning Research*, 6:1679–1704.
- Marlin, B. M., Khan, M. E., and Murphy, K. P. (2011). Piecewise bounds for estimating bernoulli-logistic latent Gaussian models. In *Proceedings of the 28th International Conference on Machine Learning*, pages 633–640.
- McLachlan, G. and Krishnan, T. (2007). *The EM Algorithm and Extensions*, volume 382. Wiley & Sons.
- Mesejo, P., Pizarro, D., Abergel, A., Rouquette, O., Beorchia, S., Poincloux, L., and Bartoli, A. (2016). Computer-aided classification of gastrointestinal lesions in regular colonoscopy. *IEEE Transactions on Medical Imaging*, 35:2051–2063.
- Minka, T. P. (2001). Expectation propagation for approximate Bayesian inference. In *Proceedings of Uncertainty in Artificial Intelligence*, volume 17, pages 362–369.
- Nishimura, A. and Suchard, M. A. (2018). Prior-preconditioned conjugate gradient for accelerated gibbs sampling in large n & large p sparse bayesian logistic regression models. *arXiv:1810.12437*.
- Pakman, A. and Paninski, L. (2014). Exact Hamiltonian Monte Carlo for truncated multivariate Gaussians. *Journal of Computational and Graphical Statistics*, 23:518–542.
- Polson, N. G., Scott, J. G., and Windle, J. (2013). Bayesian inference for logistic models using Pólya–Gamma latent variables. *Journal of the American Statistical Association*, 108:1339–1349.
- Qin, Q. and Hobert, J. P. (2019). Convergence complexity analysis of Albert and Chib’s algorithm for Bayesian probit regression. *The Annals of Statistics*, 47(4):2320–2347.
- Ray, K. and Szabó, B. (2020). Variational Bayes for high-dimensional linear regression with sparse priors. *Journal of the American Statistical Association*, pages 1–31.
- Reiß, M. (2008). Asymptotic equivalence for nonparametric regression with multivariate and random design. *The Annals of Statistics*, 36(4):1957–1982.
- Riihimäki, J., Jylänki, P., and Vehtari, A. (2013). Nested expectation propagation for Gaussian process classification with a multinomial probit likelihood. *Journal of Machine Learning Research*, 14:75–109.
- Rodriguez, A. and Dunson, D. B. (2011). Nonparametric Bayesian models through probit stick-breaking processes. *Bayesian Analysis*, 6:145–178.
- Sakar, C. O., Serbes, G., Gunduz, A., Tunc, H. C., Nizam, H., Sakar, B. E., Tutuncu, M., Aydin, T., Isenkul, M. E., and Apaydin, H. (2019). A comparative analysis of speech signal processing algorithms for Parkinson’s disease classification and the use of the tunable Q-factor wavelet transform. *Applied Soft Computing*, 74:255–263.

- Simpson, D., Rue, H., Riebler, A., Martins, T. G., and Sørbye, S. H. (2017). Penalising model component complexity: A principled, practical approach to constructing priors. *Statistical Science*, 32(1):1–28.
- Tsanas, A., Little, M. A., Fox, C., and Ramig, L. O. (2013). Objective automatic assessment of rehabilitative speech treatment in Parkinson’s disease. *IEEE Transactions on Neural Systems and Rehabilitation Engineering*, 22:181–190.
- Wang, Y. and Blei, D. M. (2019). Frequentist consistency of variational Bayes. *Journal of the American Statistical Association*, 114:1147–1161.
- Yang, Y., Pati, D., Bhattacharya, A., et al. (2020). α -variational inference with statistical guarantees. *Annals of Statistics*, 48:886–905.